Electronic Supplementary Material (ESI) for Journal of Materials Chemistry C.

Supporting Information

Flexible Metal-Organic Frameworks for Wavelength-Based Luminescence Sensing of Aqueous pH

Xiu-Liang Lv,[a] Lin-Hua Xie,[a] Bin Wang,[a] Minjian Zhao,[a] Yuanjing Cui[b] and Jian-Rong Li*[a]

[a] Beijing Key Laboratory for Green Catalysis and Separation and Department of Chemistry and Chemical Engineering, College of Environmental and Energy Engineering, Beijing University of Technology, Beijing 100124, P. R. China

[b] State Key Laboratory of Silicon Materials, Cyrus Tang Center for Sensor Materials and Applications, School of Materials Science and Engineering, Zhejiang University, Hangzhou 310027, P. R. China

*Correspondence to: jrli@bjut.edu.cn

Contents

Materials and Methods

Chemicals: All general reagents and solvents (AR grade) were commercially purchased used as received without further purification unless otherwise noticed. Zirconium tetrachloride ($ZrCl_4$), carbazole, tetrakis(triphenylphosphine) palladium ($Pd(PPh_3)_4$), methyl 6-(4,4,5,5-tetramethyl-1,3,2-dioxaborolan-2-yl)-2-naphthoate, and 4-(methoxycarbonyl)phenylboronic acid were purchased from Acros Organics. Sodium salt of caboxy methyl cellulose (CMC), potassium carbonate (K_2CO_3), iodomethane (CH_3I), cesium fluoride (CsF), acetic acid (HOAc), N,N-dimethylformamide (DMF), 1,2-dimethoxyethane (DME), chloroform ($CHCl_3$), tetrahydrofuran (THF), methanol (MeOH), ethanol (EtOH), hydrochloric acid (HCl), nitric acid (HNO_3), sulfuric acid (H_2SO_4), *p*-xylene, toluene, chlorobenzene, dichloromethane, cyclohexane, ethyl acetate, 1,4-dioxane, acetonitrile, dimethylsulfoxide (DMSO), acetone, nitromethane and nitrobenzene were bought from Sinopharm Chemical Reagent. All commercial chemicals were used as received without further purification unless otherwise noticed. All air or water sensitive reactions were carried out under a dry nitrogen atmosphere using the Schlenk technique.

Synthesis of 4,4',4'',4'''-(9*H*-carbazole-1,3,6,8-tetrayl)tetrabenzoic acid (H_4CTTB)

(1) 1,3,6,8-Tetrabromo-9*H*-carbazole (**2**)

Compound **2** was synthesized by modifying a reported procedure.[1] Commercially obtained carbazole **1** (17.00 g, 0.10 mol) was stirred in 200 mL of acetic acid (HOAc) and the solution was warmed to 30 ^{o}C. A solution of bromine (10.20 mL, 0.20 mol) in 30 mL of acetic acid was dropped in the solution over 0.5 h. The temperature of the system was then raised to 60 ^{o}C, another portion of 10.2 mL of bromine in 30 mL of acetic acid was added in the mixture. Then the mixture was stirred at 60 ^{o}C for 12 h and then cooled down to produce light-yellow solid. The crude product was recrystallized in HOAc, washed with water (3 × 100 mL) and cold ethanol (3 × 100 mL), and then dried to give pure product of **2** with a yield of 70% (33.8 g). ^{1}H NMR (400 MHz, DMSO-*d*^{6}): δ 7.88 (s, 2H, ArH), 8.53 (s, 2H, ArH), 11.66 (s, 1H, NH).

(2) Tetramethyl-4,4',4'',4'''-(9*H*-carbazole-1,3,6,8-tetrayl)tetrabenzoate (**4**)(**M$_4$CTTB**)

Compound **2** (5.00 g, 10.35 mmol) and 4-(methoxycarbonyl)phenyl)boronic acid **3** (10.24 g, 56.93 mmol) were dissolved in 320 mL of degassed ethylene glycol dimethyl ether (DME). $Pd(PPh_3)_4$ (0.60 g) and CsF (10.00 g) were then added. The reaction system was heated to reflux and stirred for 8 h under N_2 atmosphere. After the reaction completed, the mixture was cooled to room temperature. The organic solvent was evaporated and 100 mL of water was then added to the crude mixture. The solution was extracted three times with $CHCl_3$ (3 × 200 mL). The organic phase was combined and dried with $MgSO_4$ for 10 min, and evaporated to dry. The solid residue was separated by column chromatography (CH_2Cl_2 to CH_2Cl_2/EA = 10:1). Tetramethyl 4,4',4'',4'''-(9*H*-carbazole-1,3,6,8-tetrayl)tetrabenzoate **4** was isolated as a white solid (4.73 g, 65% yield based on **2**). ^{1}H NMR (400 MHz, $CDCl_3$): *δ* 3.92 (s, 12H, CH_3), 7.88 (s, 2H, ArH), 8.08 (m, 16H, ArH), 8.88 (s, 2H, ArH), 11.01 (s, 1H, NH).

(3) 4,4',4'',4'''-(9*H*-Carbazole-1,3,6,8-tetrayl)tetrabenzoic acid (**5**) (**H$_4$CTTB**)

4.73 g compound **4** was dissolved in 200 mL mixed solvent of THF and MeOH (v/v = 2:1), to which 30 mL of NaOH aqueous solution (3 N) was added. The reaction system was heated to reflux and stirred for 8 h. The clear pale yellow solution was stirred at room temperature for 2 h and the pH value was adjusted to 1 using concentrated hydrochloric acid. The resulting yellow solid was collected by filtration, and washed with water several times. The crude product was recrystallized from DMF, filtered, washed with chloroform and dried under vacuum. 3.96 g (91% yield based on **4**) product of **5** was then obtained. ^{1}H NMR (400 MHz, DMSO-*d*^{6}): *δ* 7.87 (s, 2H, ArH), 8.08 (m, 16H, ArH), 8.87 (s, 2H, ArH), 11.02 (s, 1H, NH).

Synthesis of 6,6',6'',6'''-(9*H*-carbazole-1,3,6,8-tetrayl)tetrakis(2-naphthoic acid) (H$_4$CTNA)

(1) Tetramethyl 6,6',6'',6'''-(9H-carbazole-1,3,6,8-tetrayl)tetrakis(2-naphthoate) (**7**) (**M_4CTNA**)

Compound **2** (5.00 g, 10.35 mmol) and **6** (19.40 g, 62.14 mmol) were dissolved in 320 mL of degassed DME. $Pd(PPh_3)_4$ (0.60 g, 0.52 mmol) and CsF (10.00 g, 0.065 mol) were then added. The reaction system was heated to reflux and stirred for 8 h under N_2 atmosphere. After the reaction completed, the mixture was cooled to room temperature. The organic solvent was evaporated and 100 mL of water was added to the crude mixture and the solution was extracted three times with $CHCl_3$ (3 × 200 mL). The organic phase combined and dried with $MgSO_4$ for 10 min, and evaporated to dry. The solid residue was separated by column chromatography (CH_2Cl_2 to CH_2Cl_2/EA = 5:1). Tetramethyl 6,6',6'',6'''-(9H-carbazole-1,3,6,8-tetrayl)tetrakis(2-naphthoate) **7** was isolated as a pale yellow solid (6.55 g, 70% yield based on **2**). ^{1}H NMR (400 MHz, $CDCl_3$): δ 11.20 (s, 1H, NH), 9.06 (s, 2H, ArH), 8.70 (d, 6 H, ArH), 8.60 (s, 2H, ArH), 8.07-8.33 (m, 18H, ArH), 3.95 (s, 12H, CH_3)

(2) 6,6',6'',6'''-(9*H*-carbazole-1,3,6,8-tetrayl)tetrakis(2-naphthoic acid) (**8**) (**H_4CTNA**)

6.55 g of **7** was dissolved in 200 mL mixed solvent of THF and MeOH (v/v = 2:1), to which 40 mL NaOH aqueous solution (3 N) was added. The reaction system was heated to reflux and stirred for 8 h. The clear pale yellow solution was stirred at room temperature for 2 h and the pH value was adjusted to 1 using concentrated hydrochloric acid. The resulting yellow solid was collected by filtration, and washed with water several times. The crude product was recrystallized from DMF, filtered, washed with chloroform and dried under vacuum. 5.18 g (90% yield based on **7**) the pure product of **8** was obtained.^{1}H NMR (400 M Hz, DMSO-d^6): δ 13.09 (s, 4H), 11.20 (s, 1H), 9.03 (s, 2H), 8.70 (d, 6 H), 8.60 (s, 2 H), 8.03-8.31 (m, 18 H).

Synthesis of $[Zr_6O_4(OH)_8(H_2O)_4(CTTB)_2]$ (BUT-62W). $ZrCl_4$ (56 mg, 0.24 mmol), H_4CTTB (78 mg, 0.12 mmol), and acetic acid (4.0 mL) in 10 mL of DMF were mixed and ultrasonically dissolved in a 20 mL Pyrex vial. The resulting mixture was sealed and heated at 120 °C for 24 h. After cooling down to room temperature, block crystals of BUT-62W were harvested by filtration (60 mg, 58% yield based on $ZrCl_4$). EA calcd (%) for $Zr_6O_{38.5}H_{99}C_{97}N_{7.5}$: C 45.99, N 4.15, H 3.94. Found: C 45.68, N 3.99, H 4.09. FT-IR spectrum of as-synthesized BUT-62W is shown in Figure S2, and TGA curve is shown in Figure S6a.

Synthesis of [$Zr_6O_4(OH)_8(H_2O)_4$(CTTB-CH_3)$_2$] (BUT-62W-CH_3). As-synthesized BUT-62W (50 mg, 0.047 mmol), iodomethane (0.031 mL, 0.50 mmol), and K_2CO_3 (0.069 g, 0.5 mmol) were added into a 50 mL three-neck bottle filled with 20 mL of DMF, then the mixture was heated and stirred at 40 °C for 3 d. After cooling down to room temperature, the crystal was filtered and washed with DMF. The obtained material is referred as BUT-62W-CH_3. EA calcd (%) for $Zr_6O_{37}H_{94.5}C_{95.5}N_{6.5}$: C 46.39, N 3.68, H 3.85. Found: C 45.98, N 3.89, H 4.01. H_4CTTB-CH_3 ligand was obtained from the decomposition of BUT-62W-CH_3 in basic aqueous solution: as-synthesized BUT-62W-CH_3 (30 mg) was dissolved in 20 mL of NaOH (5 M) aqueous solution. After filtration, 10 mL of HCl (2 M) aqueous solution was added in the resulting solution and the solid was separated by filtration. ^{1}H NMR was recorded to identify the ligand (SI, Figure S28).

Synthesis of [$Zr_6O_4(OH)_8(H_2O)_4$(CTNA)$_2$] (BUT-63W). $ZrCl_4$ (30 mg, 0.129 mmol), H_4CTNA (50 mg, 0.06 mmol), and formic acid (3.5 mL) in 10 mL of DMF were mixed and ultrasonically dissolved in a 20 mL Pyrex vial. The resulting mixture was sealed and heated at 100 °C for 48 h. After cooling down to room temperature, block crystals of BUT-63W were harvested by filtration (60 mg, 78% yield based on $ZrCl_4$). EA calcd (%) for $Zr_6O_{41}H_{123.5}C_{101.0}N_{8.5}$: C 52.21, N 3.90, H 4.13. Found: C 52.53, N 3.62, H 4.40. FT-IR spectrum of as-synthesized BUT-63W is shown in Figure S3, and TGA curve is shown in Figure S6b.

Detailed sample activation and gas adsorption of BUT-62 and -63, stability test of BUT-62 and -63, N_2 adsorption of acid or base treated BUT-62 and -63, temperature-dependent PXRD of BUT-62 and -63, fluorescence measurements for pH sensing and molecule recognition, fabrication of MOF/CMC plates can be found in SI.

Single-Crystal X-ray Diffraction Structure Analysis of BUT-62 and -63. The diffraction data of BUT-62W, -62Y, -62W-CH_3, and -63W were collected in a Rigaku Supernova CCD diffractometer equipped with a mirror-monochromatic enhanced Cu-K_α radiation (λ = 1.54184 Å) at 100 K. The data sets were corrected by empirical absorption correction using spherical harmonics, implemented in the SCALE3 ABSPACK scaling algorithm.[2] The structures were solved by direct methods and refined by full-matrix least-squares on F^2 with anisotropic displacement by using the SHELXTL software package.[3] Non-hydrogen atoms on the frameworks were refined with anisotropic displacement parameters during the final cycles. Hydrogen atoms of ligands were calculated in ideal positions with isotropic displacement parameters. Those in −OH/H_2O groups of the Zr(IV)-based clusters were not added but were calculated into molecular formula of the crystal data. There are large solvent accessible pore volumes in the structures of BUT-62W and -63W, which are occupied by highly disordered solvent molecules. No satisfactory disorder model for these solvent molecules could be achieved, and therefore the SQUEEZE program implemented in PLATON was used to remove these electron densities of these disordered species.[4] Thus, all of electron densities from free solvent molecules have been "squeezed" out. For BUT-62Y, partial strongly adsorbed water molecules could be modelled. A partially water included structure as well as a squeezed structure for BUT-62Y are also provided. The details of crystal data and structural refinement can be found in Table 1-5 of the Supplementary Information, and the provided CIF files.

Sample Activation and Gas Adsorption of BUT-62 and -63. In each case, as-synthesized sample (about 100 mg) obtained through the solvothermal reaction was immersed in fresh DMF (30 mL) at 60 °C for 24 h to remove unreacted starting ligands and inorganic species. For the optimization of activation procedure, 2 mL of 2 M HCl aqueous solution was added to the DMF suspension of BUT-62W. Afterwards, extract was carefully decanted and the sample was washed with DMF (20 mL) and acetone (30 mL) for one time, separately. After being further soaked in acetone (50 mL) for another 24 h, the sample was collected and activated at 40 °C under vacuum for 12 h, resulting the activated phase of BUT-62, $[Zr_6O_4(OH)_8(H_2O)_4(CTTB)_2]$ (**BUT-62A**) or activated $[Zr_6O_4(OH)_8(H_2O)_4(CTNA)_2]$ (**BUT-63A**). Then, gas or vapor adsorption isotherms were recorded at 77 K (N_2), 87 K (Ar), 195 K (CO_2), or 298 K (vapor of methanol or water).

Stability Test of BUT-62 and -63 through PXRD. Activated samples BUT-62A and -63A (about 10 mg in each) were immersed in about 3 mL of water, 2 M HCl, and pH = 9 NaOH aqueous solution at room temperature for 24 h, respectively. PXRD patterns were then recorded after the treated samples were collected by filtration.

N_2 Adsorption of Acid or Base Treated BUT-62 and -63. Activated samples BUT-62A and -63A (about 100 mg for each) were firstly immersed in 35 mL of 2 M HCl aqueous solution and pH = 9 NaOH aqueous solution at room temperature for 24 h, respectively. After being filtered and washed with excess of water, the samples were further immersed in 200 mL of acetone at 40 °C for 12 h. Then the samples were collected, dried in air, and degassed for 10 h at 100 °C before the N_2 adsorption at 77 K.

Temperature-Dependent PXRD of BUT-62 and -63. As-synthesized BUT-62W and -63W samples (about 10 mg for each) were used to perform the temperature-dependent PXRD under N_2 atmosphere. The temperature-increasing rate was set as 10 °C/min. The measurement was performed from 293 to 543 K in each case. The PXRD patterns recorded at 293, 373, 443, and 543 K, respectively, are shown in Figure S7 and 8. To check whether the structural transformations of the two MOFs are reversible, the samples after being heated at 543 K were immersed in a mixture of 20 mL DMF and 0.5 mL of 2 M HCl aqueous solution for 5 min and 1 h, respectively. After being filtrated, the samples were collected for PXRD measurements.

Fluorescence Measurements for pH Sensing. In a typical experiment for pH sensing, 10 mg of BUT-62Y (or BUT-63Y) sample was weighed and then slightly grounded. The resulting sample was added into to a cuvette containing 2 mL liquid (aqueous solutions with different pH values or different solvents). The mixture was stirred at a constant rate for 1 min to maintain its homogeneity before fluorescence measurement. The fluorescence was then recorded at room temperature. Each measurement was repeated three times, and the average value of λ_{max} was used for linear fitting of the data.Fresh sample was used for each cycle test, and the same sample was reused to test multiple pH values. After the fluorescence measurement, the sample was collected by centrifugation and washed with deionized water. Ultrapure water with tested pH = 7 was used. A acidic or basic aqueous solution was firstly prepared by mixing about 100 μL of concentrated HCl or NaOH aqueous solution with about 10 mL deionized water. Then the aqueous solutions with different pH values were obtained from diluting the as-made acidic or basic solution with deionized water (with the aid of a pH meter to check the pH value). All aqueous solutions were used just as they were freshly prepared.

Fabrication of MOF/CMC plates. BUT-62Y or BUT-63Y (about 2.0 g) was added into an aqueous solution of CMC (20 mL, 3% concentration). The mixture was stirred until a uniform suspension formed. A small amount of suspension was then carefully poured on a glass slide, and the glass slide was tilted carefully from side to side until the suspension covered all surface of the plate as a homogenous thin layer. The plate was then dried in air for 24 h before use.

Supplementary Schemes

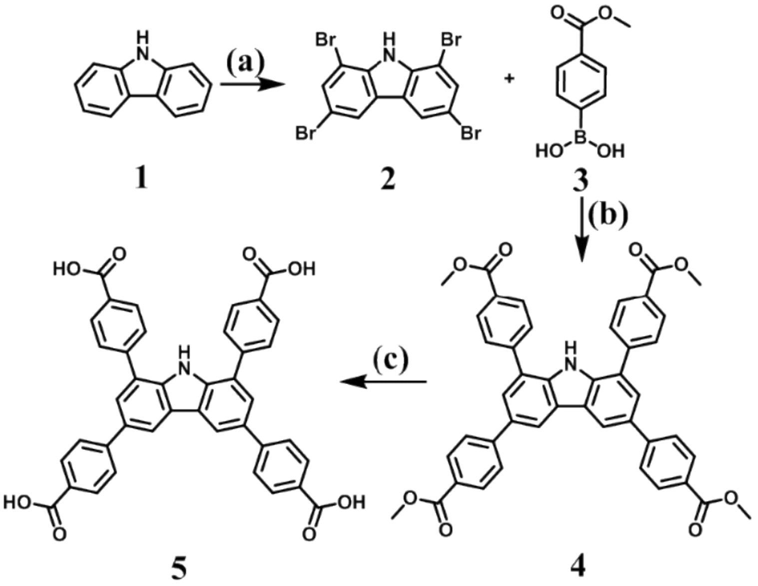

Scheme S1. Synthesis of H_4CTTB. (a) Br_2, HOAc, 60 °C; (b) CsF, $Pd(PPh_3)_4$, DME, Reflux; (c) THF/MeOH, NaOH aqueous, Reflux.

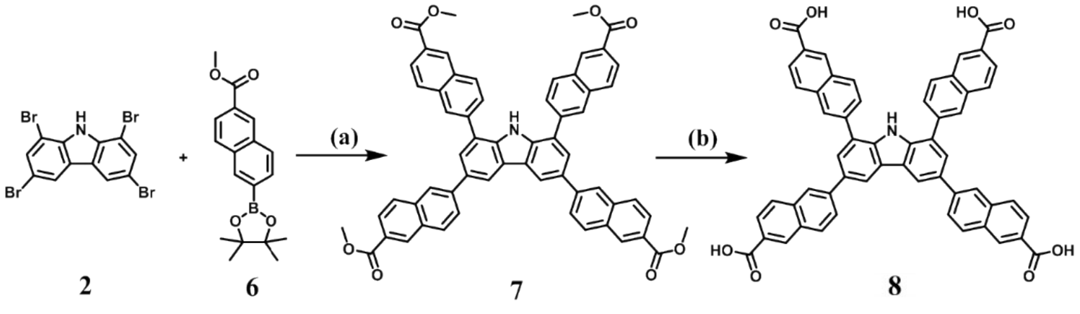

Scheme S2. Synthesis of H_4CTNA. (a) CsF, $Pd(PPh_3)_4$, DME, Reflux; (b) THF/MeOH, NaOH aqueous, Reflux.

Supplementary Figures

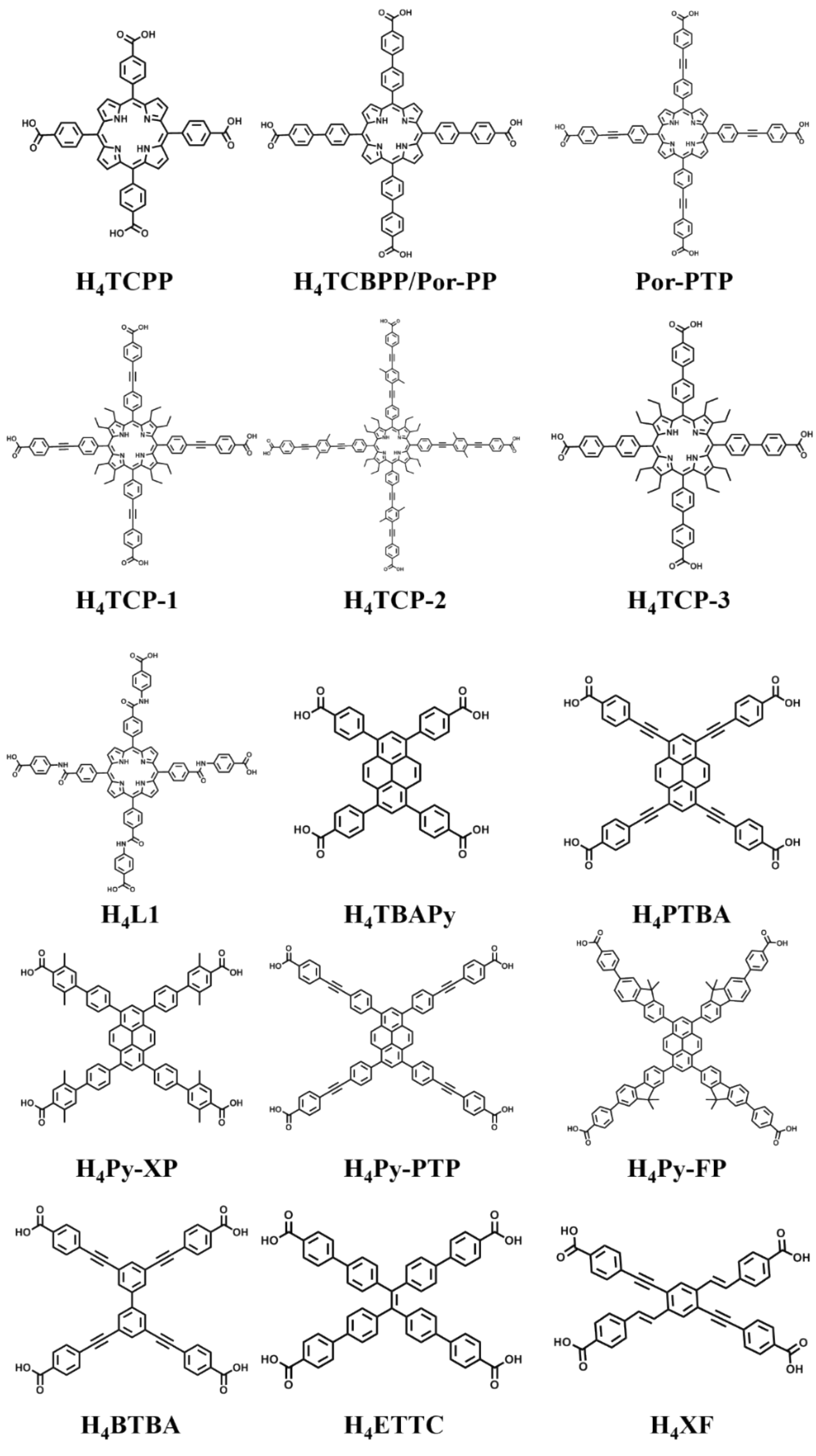

Figure S1. Planar tetratopic carboxylate ligands used in reported Zr-MOFs.

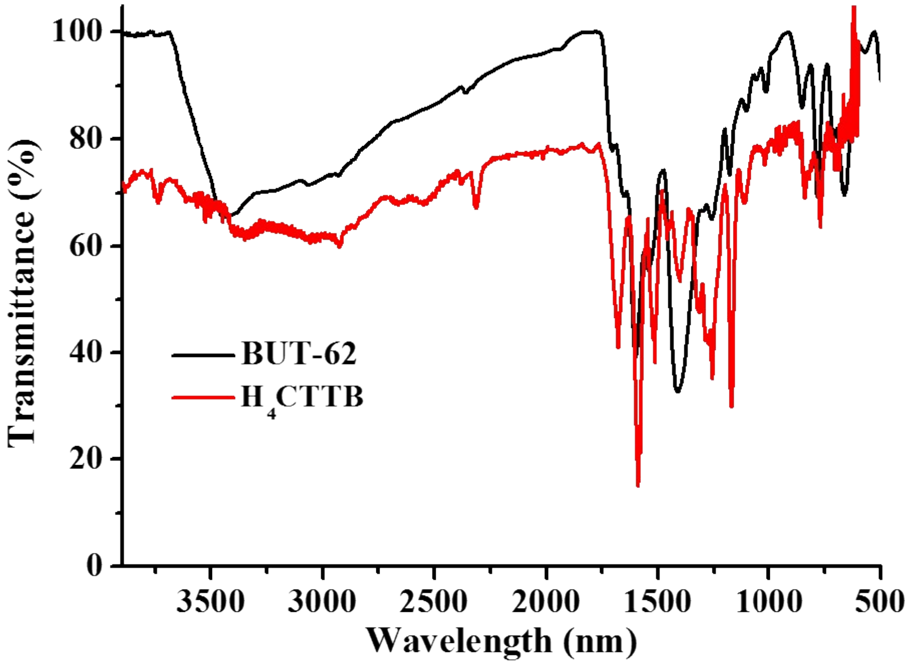

Figure S2. FT-IR spectra of BUT-62W and ligand H_4CTTB.

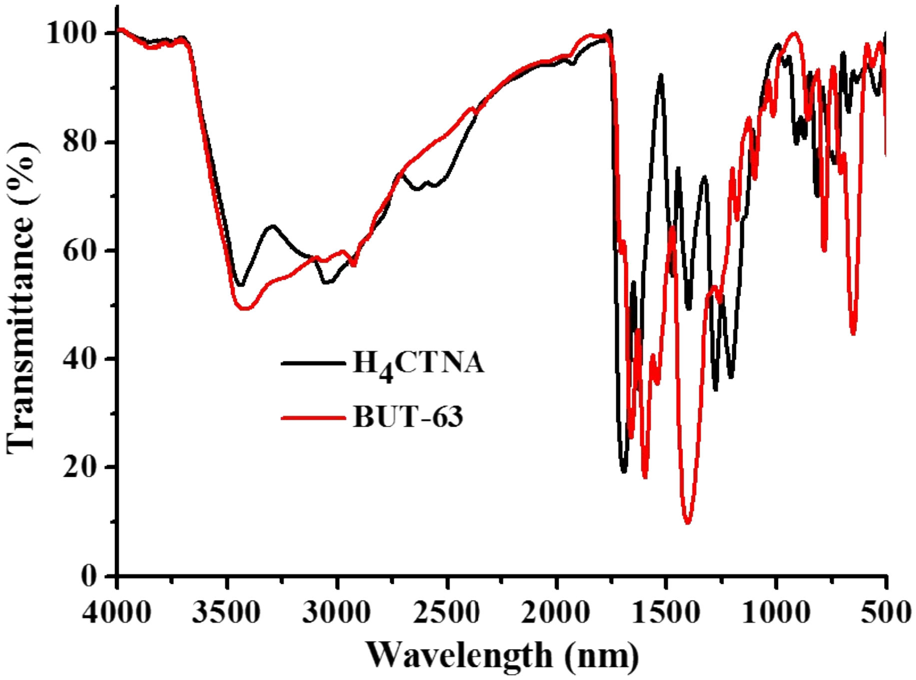

Figure S3. FT-IR spectra of BUT-63W and ligand H_4CTNA.

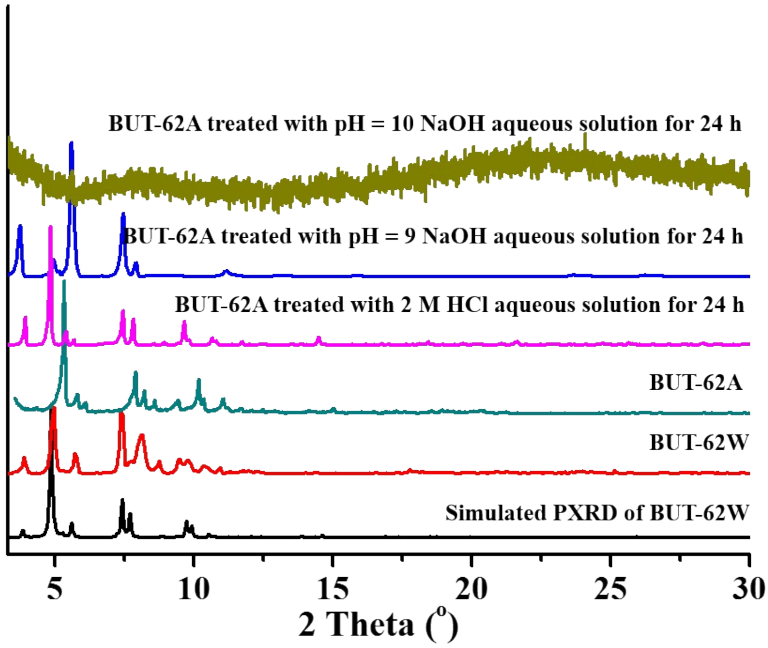

Figure S4. PXRD patterns of BUT-62 samples treated under different conditions to check its chemical stability.

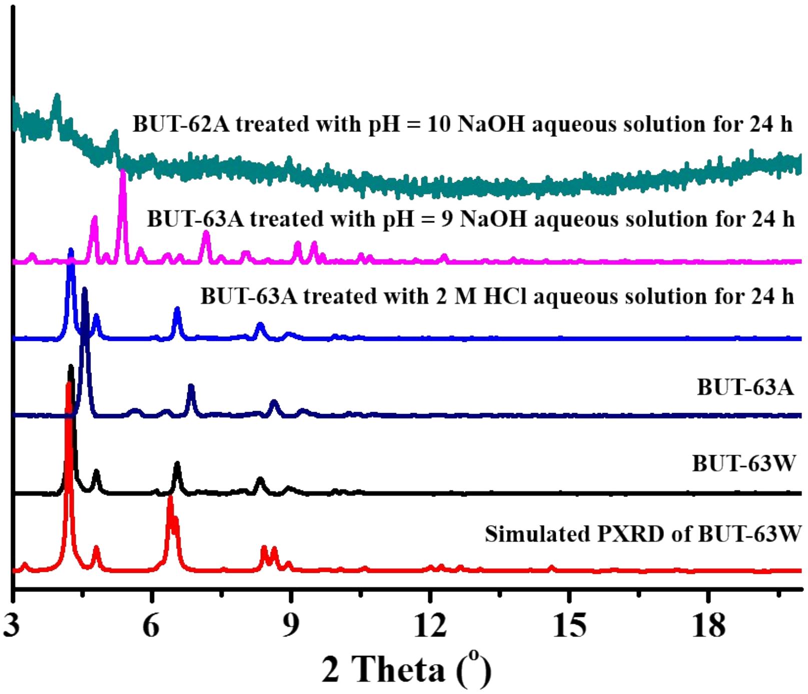

Figure S5. PXRD patterns of BUT-63 samples treated under different conditions to check its chemical stability.

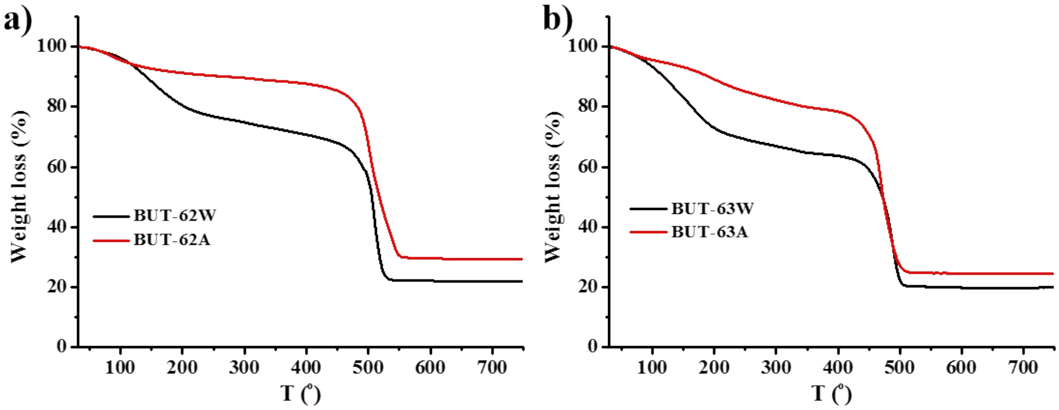

Figure S6. TGA curves of BUT-62W, -62A, -63W, and -63A recorded under the atmosphere of open air.

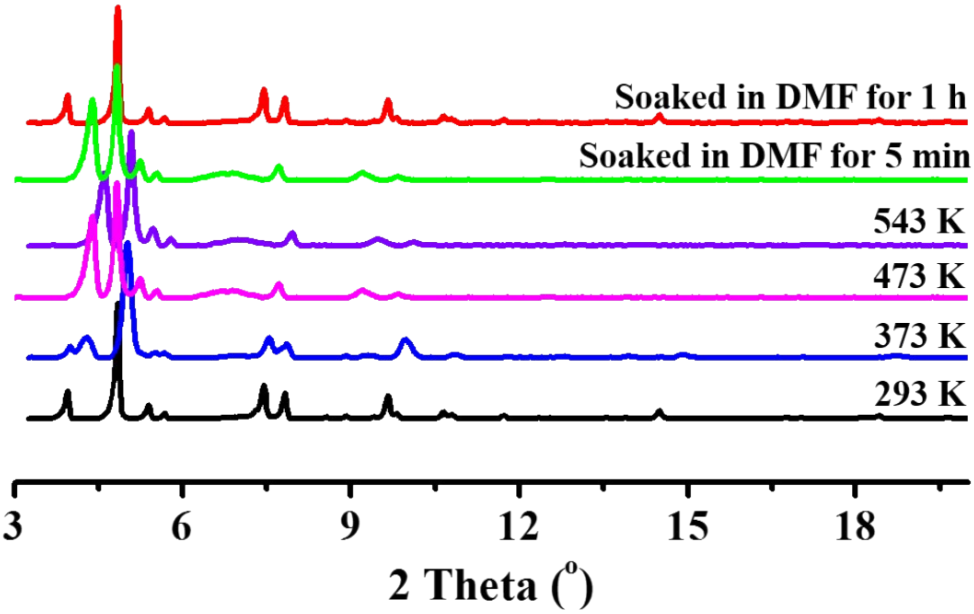

Figure S7. Temperature-dependent PXRD patterns of BUT-62W and PXRD patterns for the sample after heated at 543 K and subsequently immersed in acidic DMF.

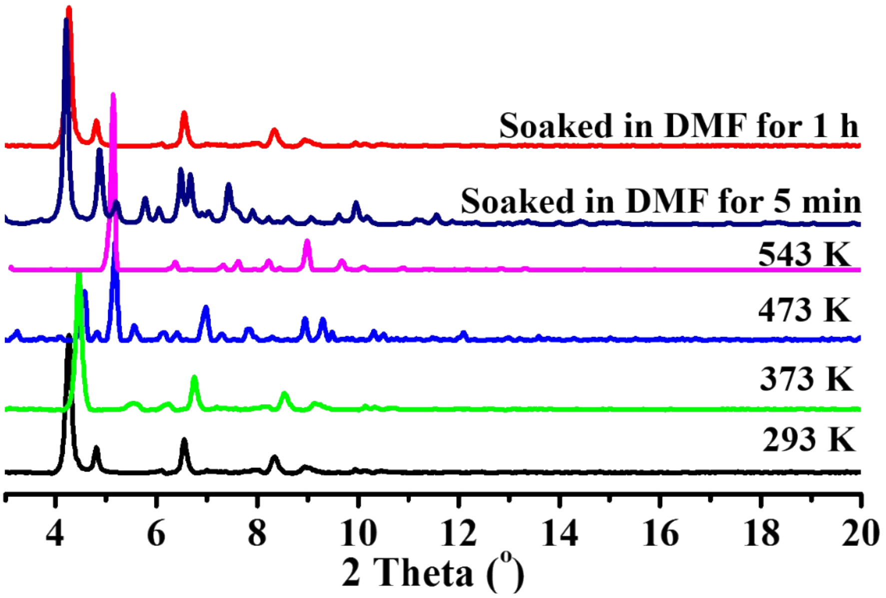

Figure S8. Temperature-dependent PXRD patterns of BUT-63W and PXRD patterns for the sample after heated at 543 K and subsequently immersed in acidic DMF.

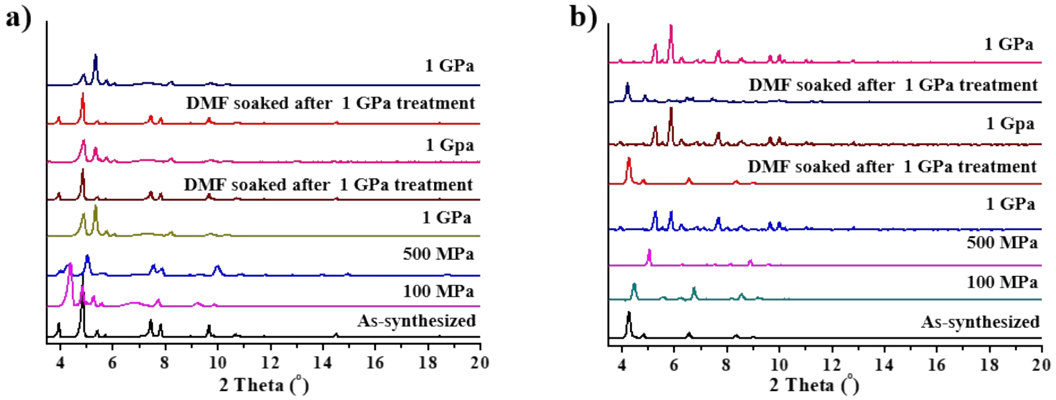

Figure S9. Pressure-dependent PXRD patterns of BUT-62(a), BUT-63(b) and PXRD patterns for the sample after compressed under 1GPa and subsequently immersed in acidic DMF.

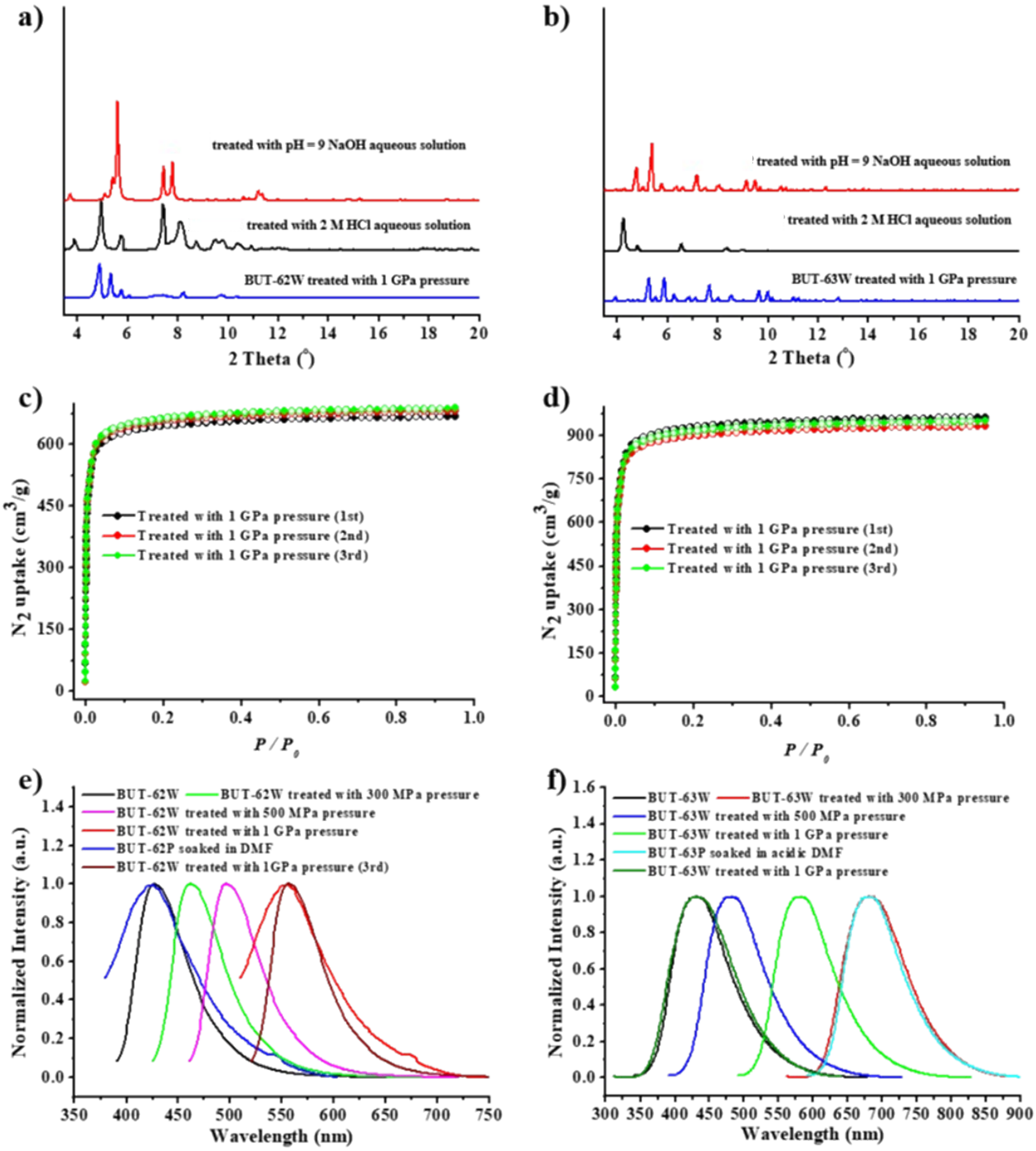

Figure S10. The PXRD pattern of BUT-62 (a) and -63 (b) after different treatments and N_2 isotherms and fluorescence spectra of BUT-62 (e) and -63 (f) recorded in repeat tests for 3 cycles.

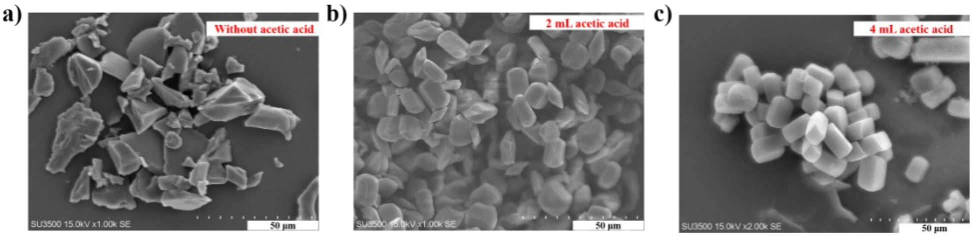

Figure S11. SEM image of BUT-62W samples synthesized with (a) 0 mL, (b) 2 mL, and (c) 4 mL acetic acid, respectively.

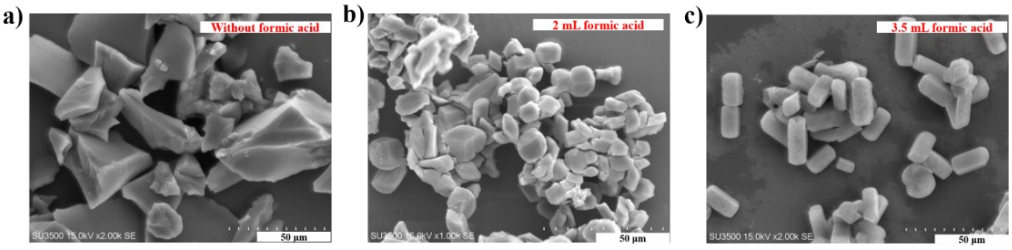

Figure S12. SEM image of BUT-63W samples synthesized with (a) 0 mL, (b) 2 mL, and (c) 3.5 mL formic acid.

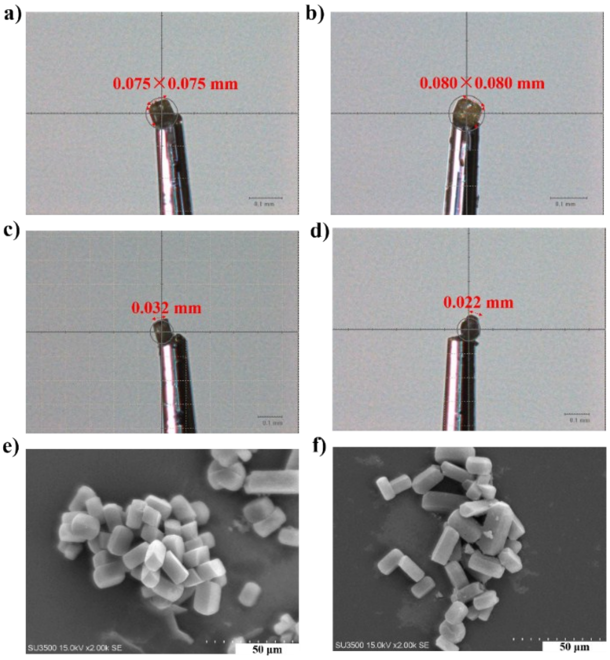

Figure S13. Optical photographs of a BUT-62W single crystal (a and c) and the single crystal transformed into BUT-62Y (b and d) viewing along different directions; (e, f) SEM images of bulk samples of BUT-62W (e) and BUT-62Y (f), respectively.

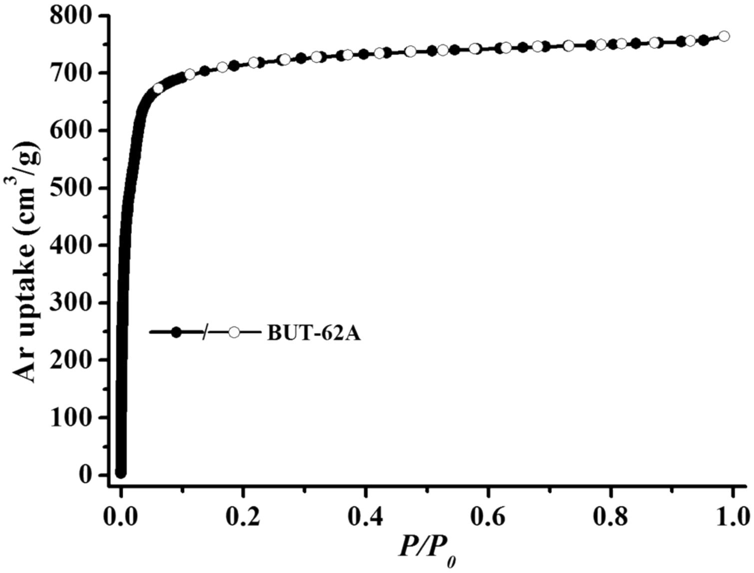

Figure S14. Ar adsorption/desorption isotherms of BUT-62A at 87 K.

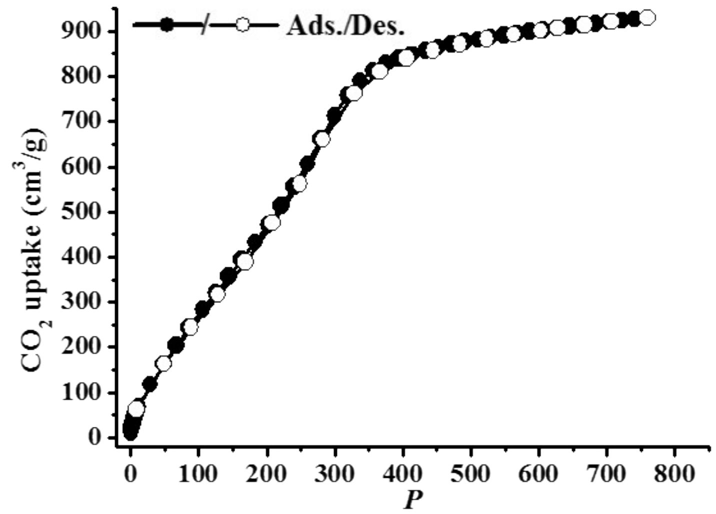

Figure S15. CO$_2$ adsorption/desorption isotherms of BUT-62A at 195 K.

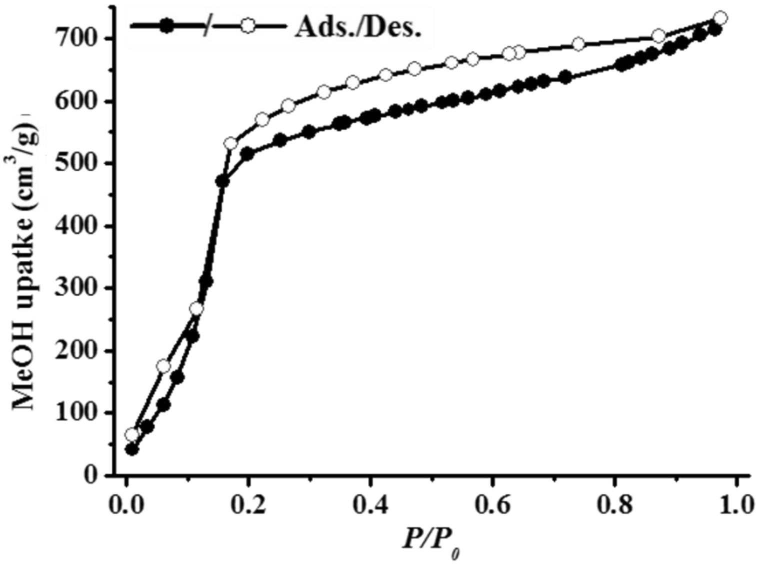

Figure S16. MeOH vapor adsorption/desorption isotherms of BUT-62A at 298 K.

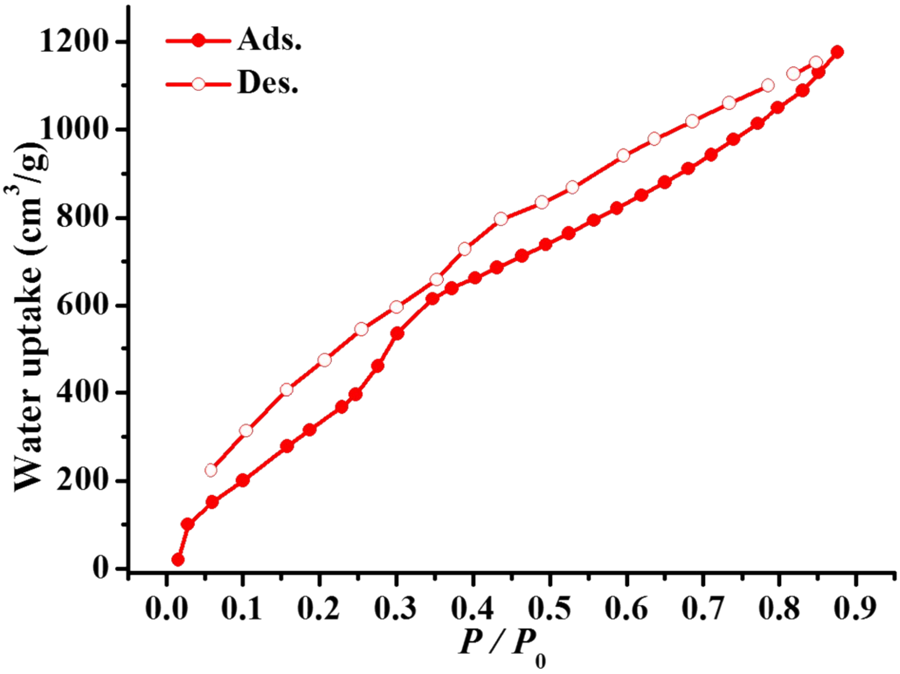

Figure S17. Water adsorption-desorption isotherms of BUT-62A recorded at 298 K.

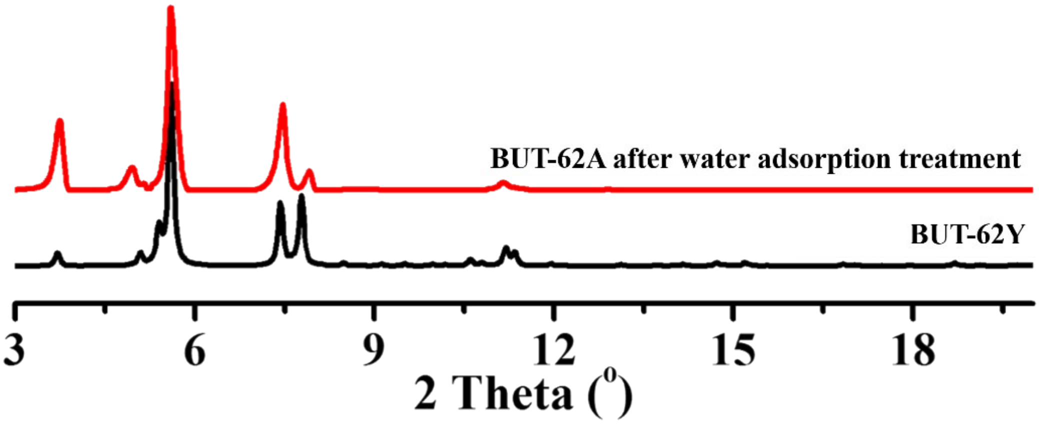

Figure S18. PXRD pattern of the sample of BUT-62A after water adsorption and the simulated PXRD pattern of BUT-62Y.

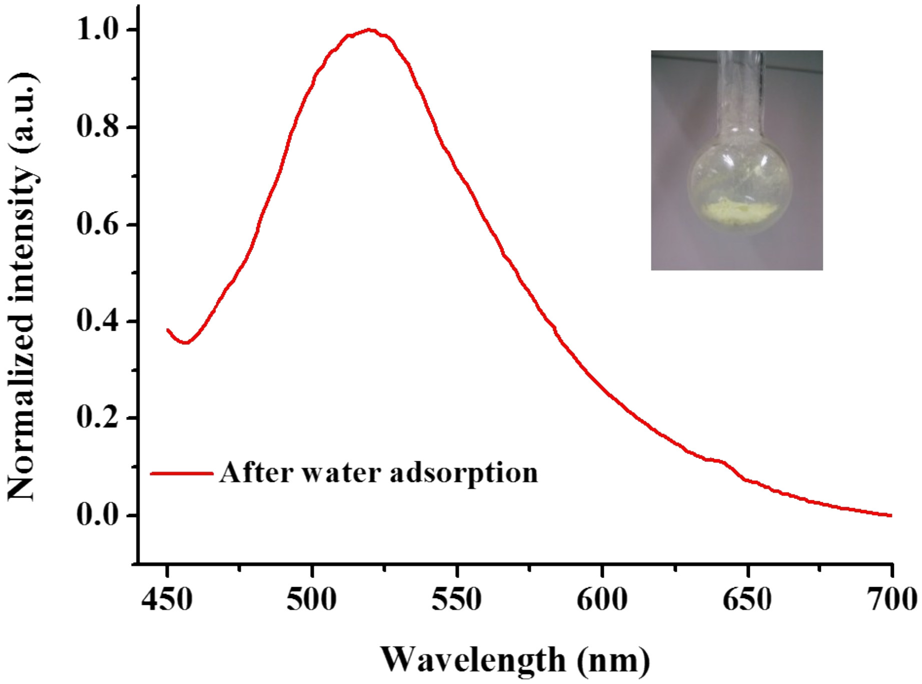

Figure S19. Fluorescent emission (upon excitation at 370 nm) and optical photographof the sample of BUT-62A after water adsorption.

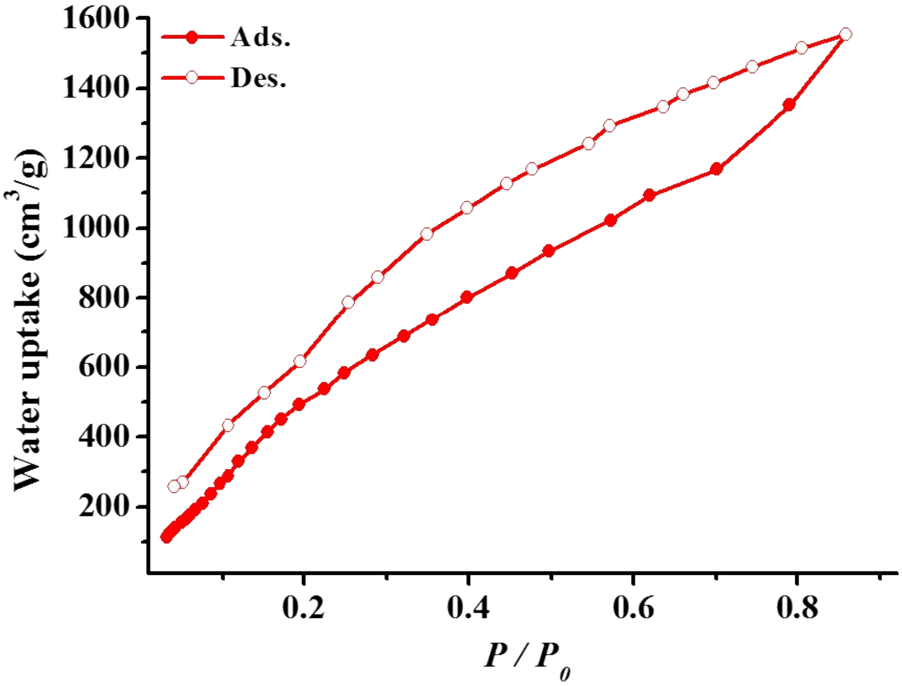

Figure S20. Water adsorption-desorption isotherms of BUT-63A recorded at 298 K.

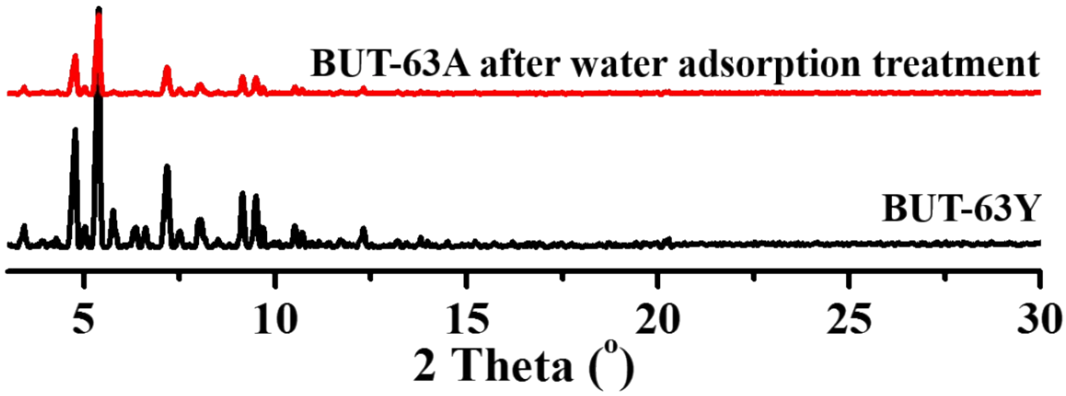

Figure S21. PXRD patterns of the sample of BUT-63A after water adsorption and a sample of BUT-63Y.

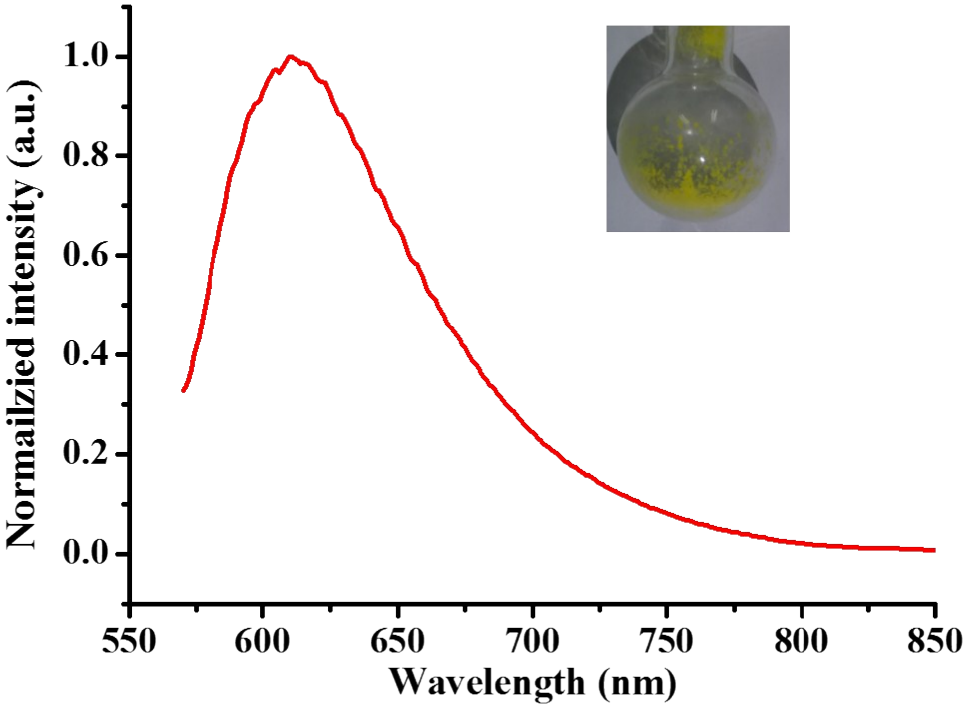

Figure S22. Fluorescent emission (upon excitation at 375 nm) and optical photographof the sample of BUT-63A after water adsorption.

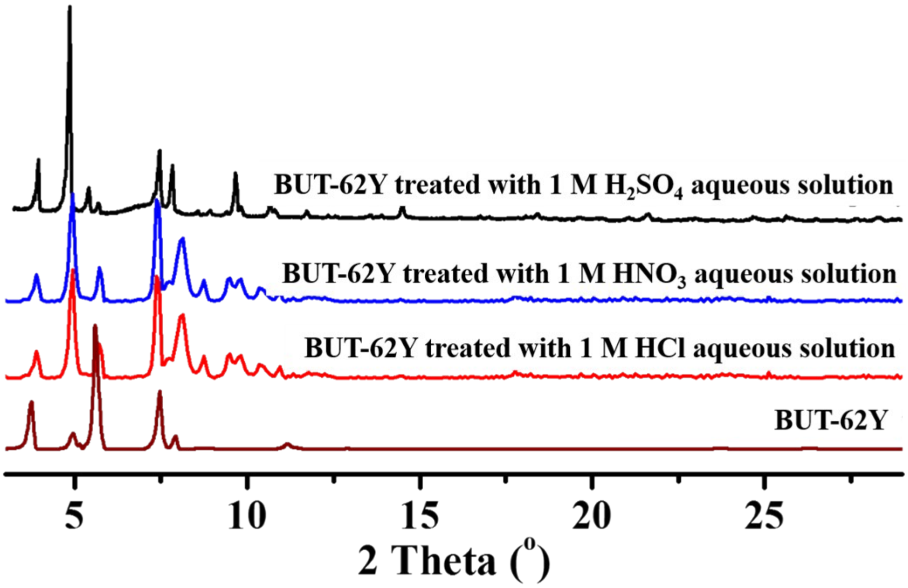

Figure S23. The PXRD patterns of BUT-62 samplesafter being treated with strong acids with different anions.

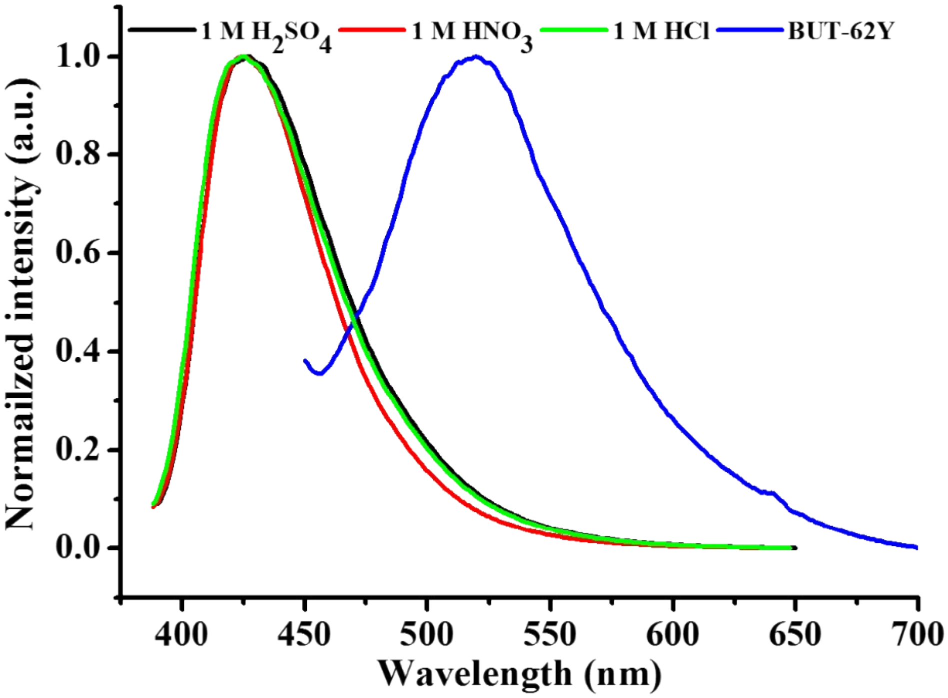

Figure S24. Intensity-normalized luminescent spectra of BUT-62Y, and BUT-62 samples after being treated with strong acids with different anions.

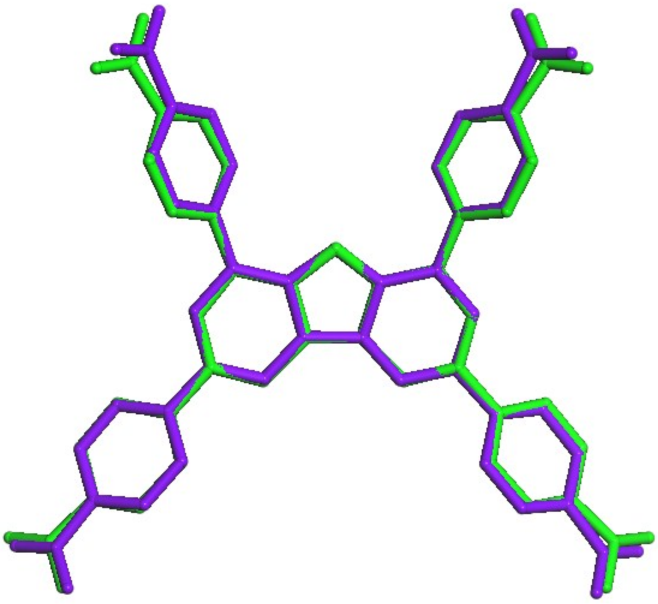

Figure S25. Superposed view of theCTTB^{4-} ligands inBUT-62W (purple bond) and inBUT-62Y (green bond).

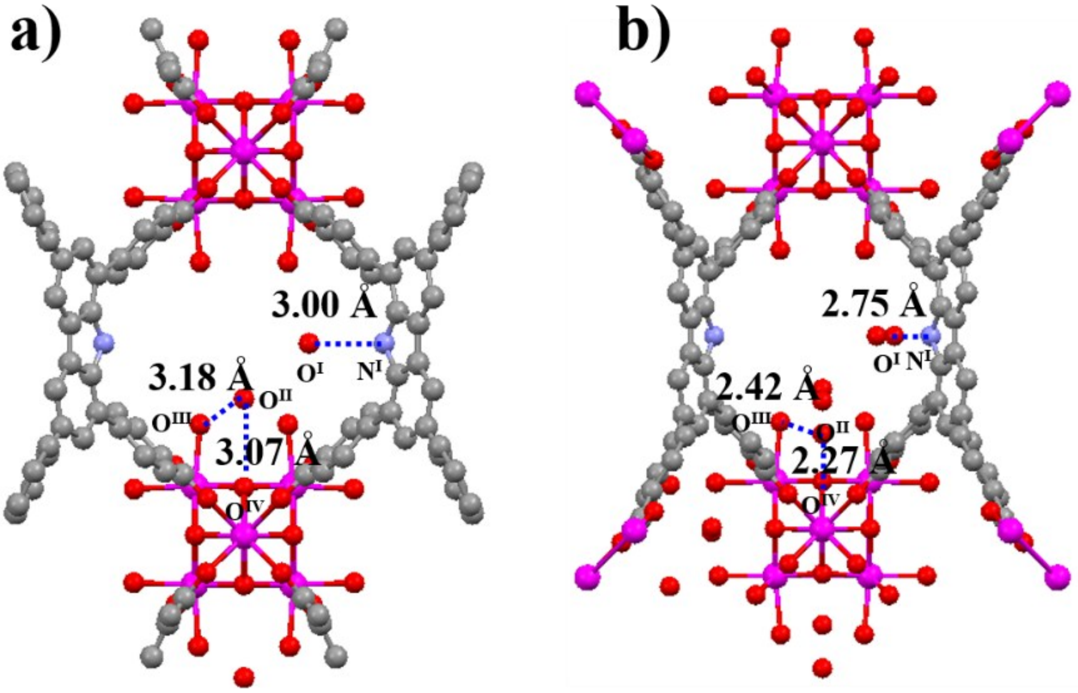

Figure S26. H-bonding donors and acceptors, as well as the distances between these atoms in BUT-62W (a) and BUT-62Y (b), respectively.

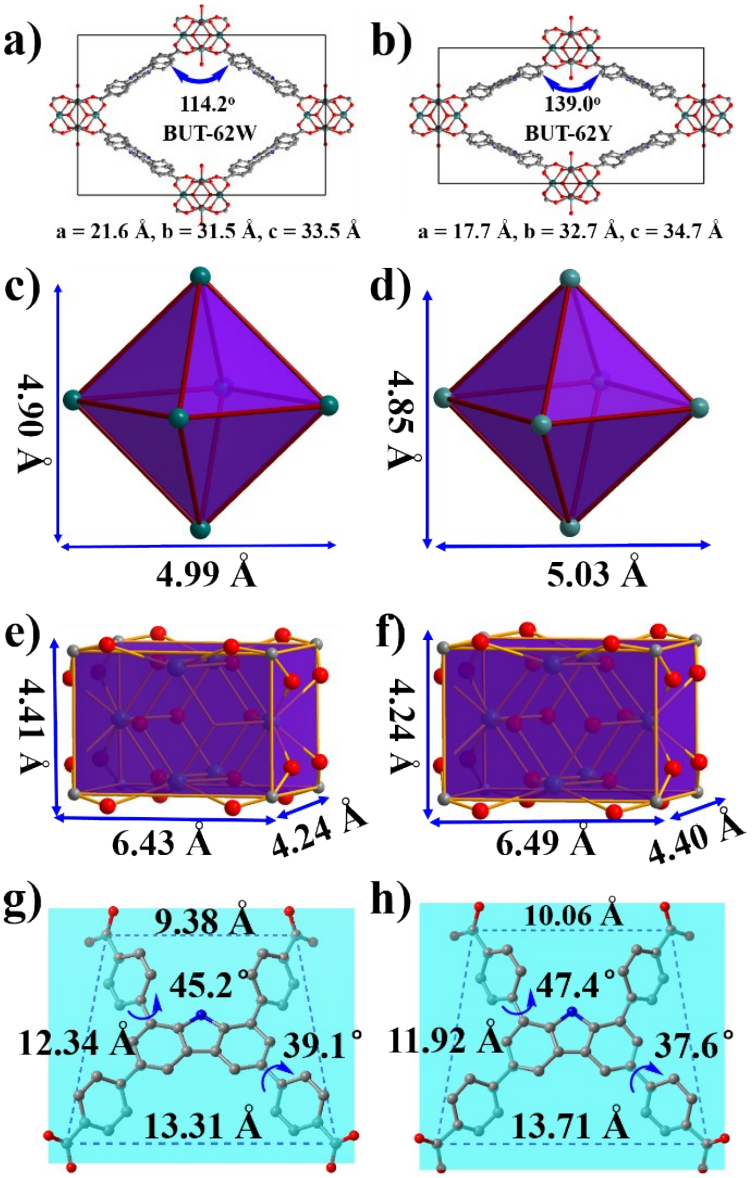

Figure S27. Comparison of the structural details between BUT-62W (left) and BUT-62Y (right):Intensity normalized luminescent spectra of BUT-62 (a) and -63 (b) treated in aqueous solutions with different pH values at room temperature; c) the pH dependence of the wavelength of emission maximum (λ_{max}) and the linear fits for BUT-62 (red) and -63 (black); and photographs of BUT-62Y/CMC plate (d) and BUT-63Y/CMC plate (e) under 365 nm UV irradiation after being dipped in aqueous solutions with different pH values. (a, b) unit cell parameters and pore shape, (c, d) size of the Zr_6 octahedron cluster, (e, f) cuboid-shaped $[Zr_6(\mu_3\text{-}O)_4(\mu_3\text{-}OH)_4(OH)_4(-COO)_8]$ SBU, and (g, h) $CTTB^{4-}$ linker geometry (color code: Zr, green; C, gray; O, red; and N, blue).

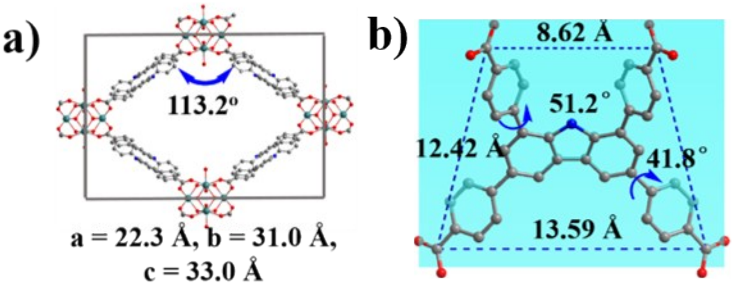

Figure S28. (a) Unit cell parameters and pore shape, and (b) CTTB^{4-} linker geometry (color code: Zr, green; C, gray; O, red; and N, blue) for BUT-62@Toluene.

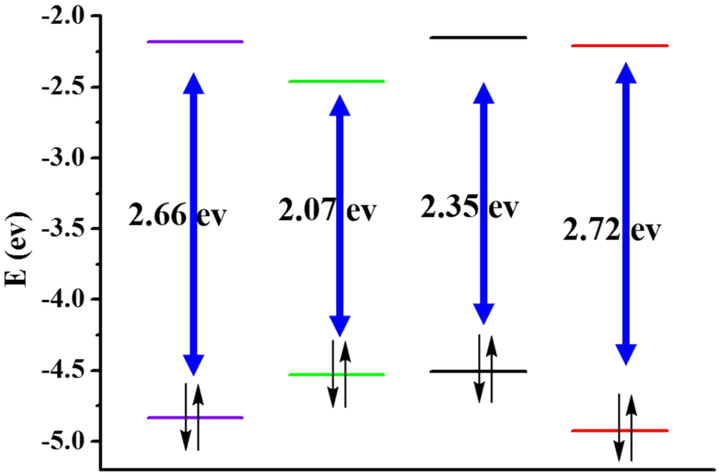

Figure S29. HOMO and LUMO energies for H_4CTTB ligand derived from Toluene@BUT-62 (red line), BUT-62W (purple line), BUT-62Y (green line), and optimized (black line) free ligand, respectively.

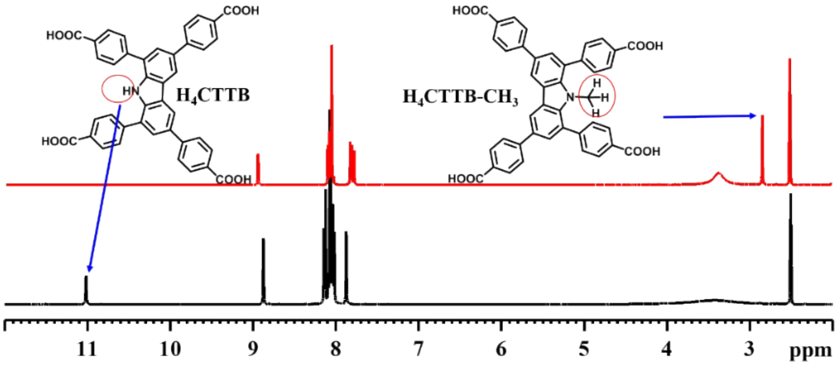

Figure S30. Comparison of ^{1}H NMR spectra of H_4CTTB and $H_4CTTB\text{-}CH_3$.

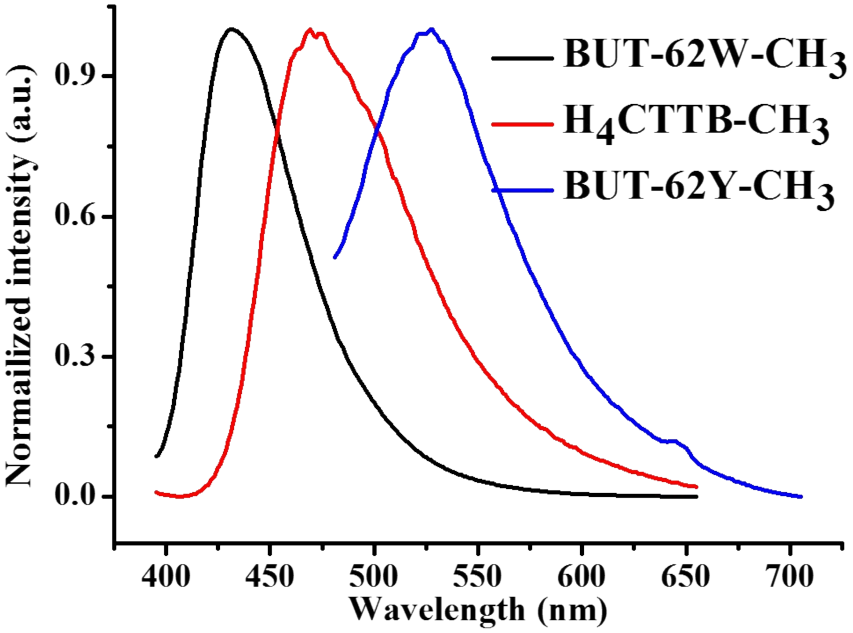

Figure S31. Intensity normalized luminescent spectra of BUT-62W-CH_3, -62Y-CH_3, and H_4CTTB-CH_3 in solid state.

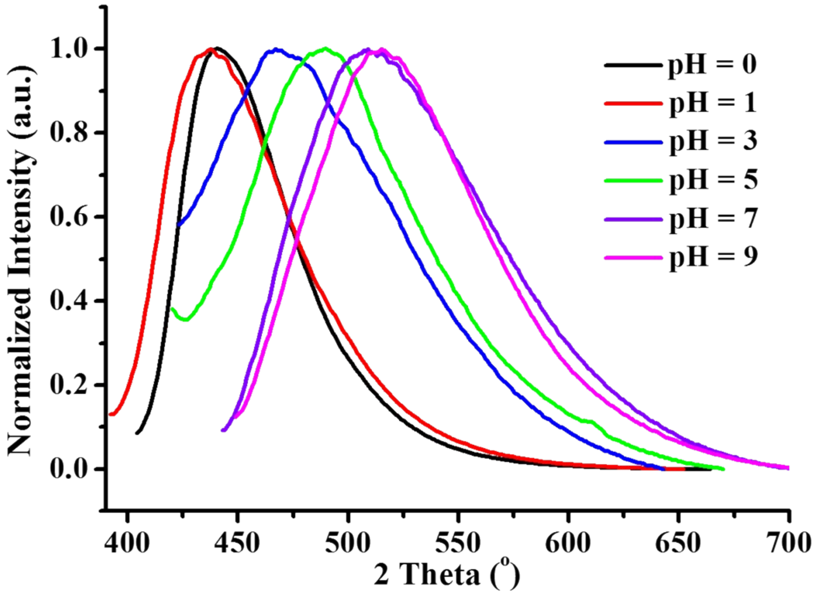

Figure S32. Intensity normalized luminescent spectra of BUT-62-CH_3 treated in aqueous solutions with different pH values at room temperature.

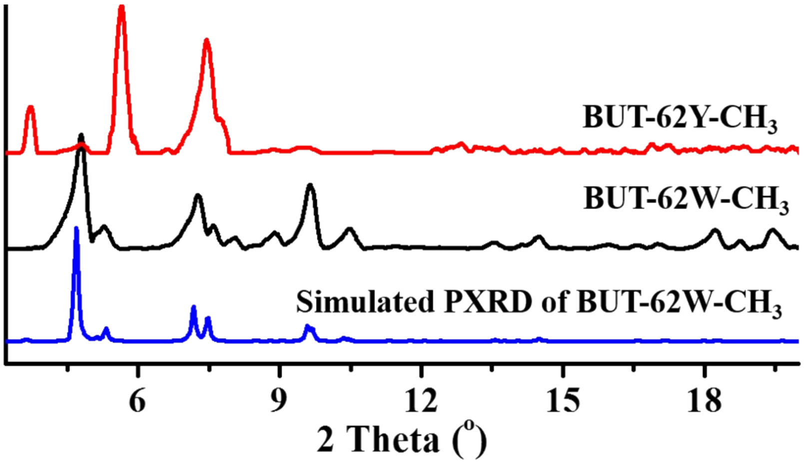

Figure S33. Comparison of simulated PXRD of BUT-62W-CH$_3$ and experimental PXRD patterns ofBUT-62Y-CH$_3$ and BUT-62W-CH$_3$.

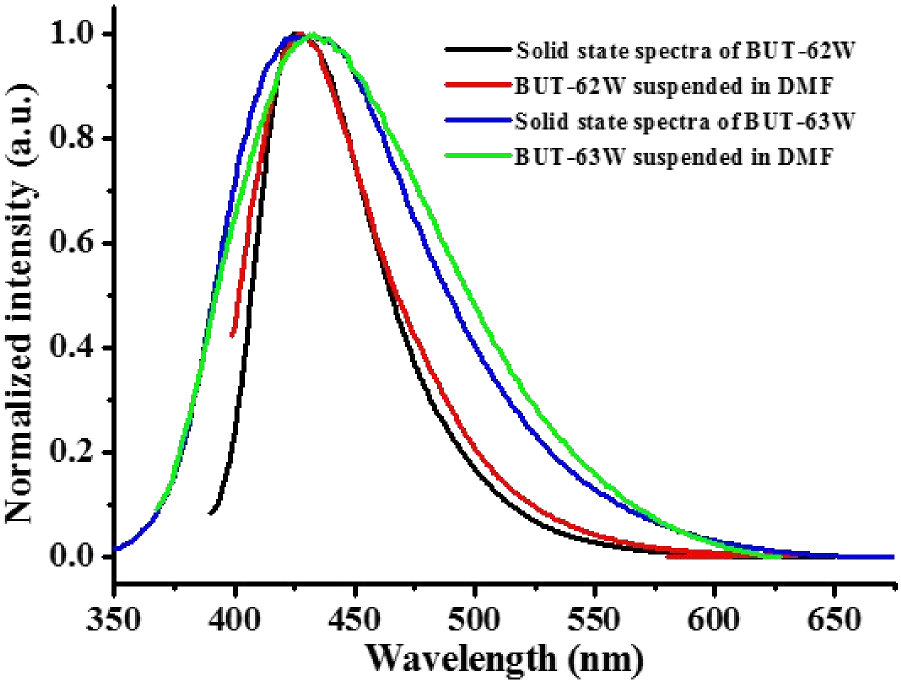

Figure S34. Solid state fluorescence spectra for BUT-62W and -63W, and fluorescence spectra for BUT-62W and -63W suspended in DMF, respectively.

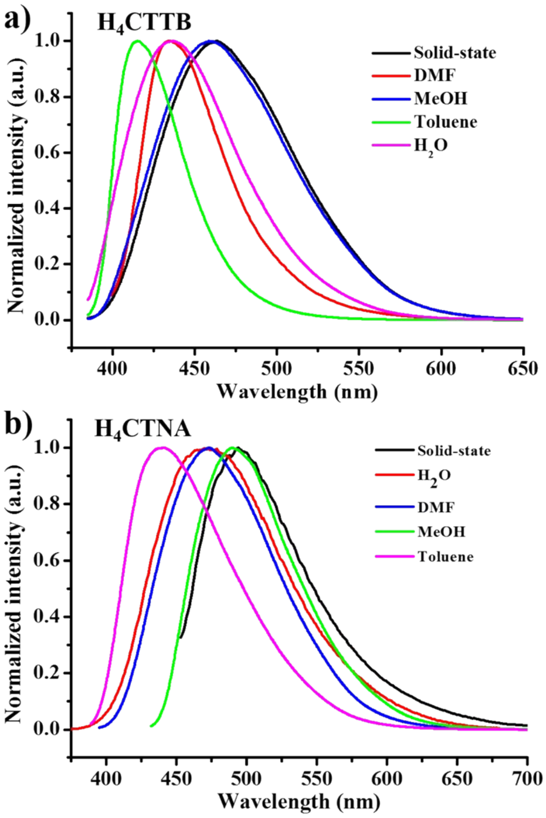

Figure S35. Fluorescence spectra of the ligands H_4CTTB (a) and H_4CTNA (b) in solid state and the ligands dissolved in DMF, water, methanol, and toluene, respectively.

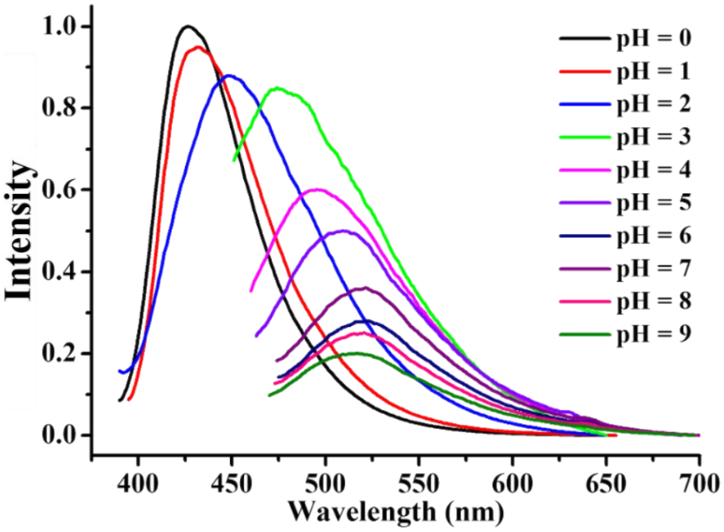

Figure S36. Emission spectra of BUT-62 after suspended in aqueous solutions with different pH values upon the excitation at 370 nm.

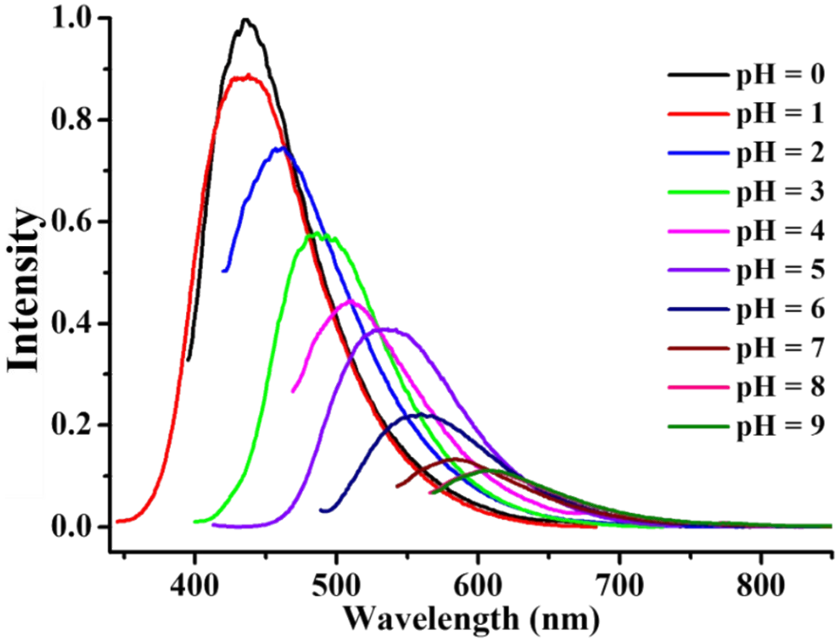

Figure S37. Emission spectra of BUT-63 after suspended in aqueous solutions with different pH values upon the excitation at 375 nm.

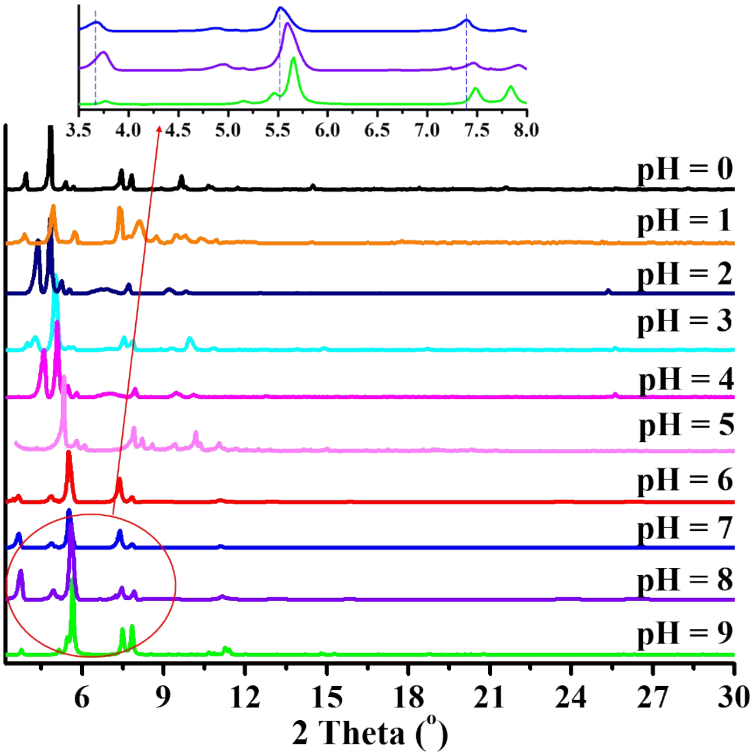

Figure S38. PXRD patterns of BUT-62 samples treated in aqueous solutions with different pH values at room temperature.

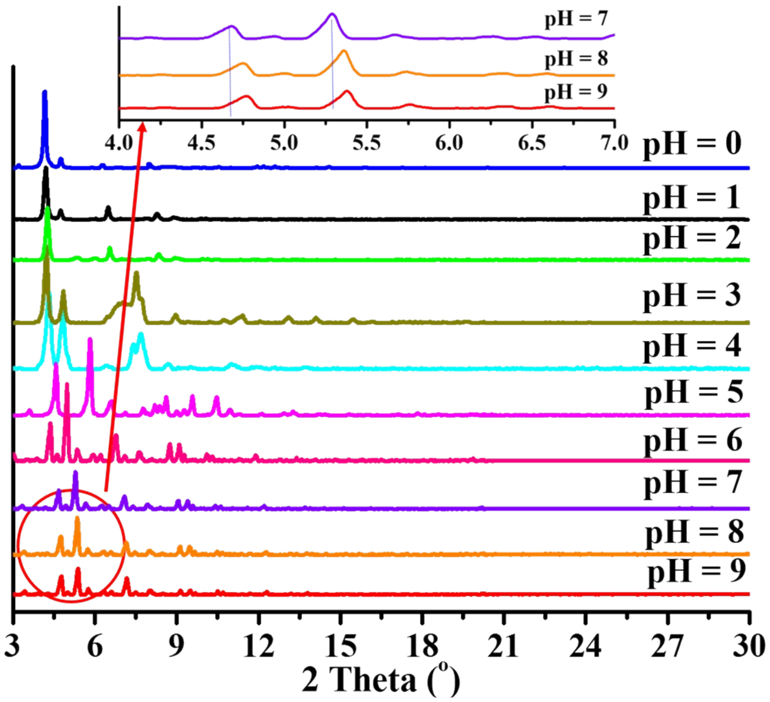

Figure S39. PXRD patterns of BUT-63 samples treated in aqueous solutions with different pH values at room temperature.

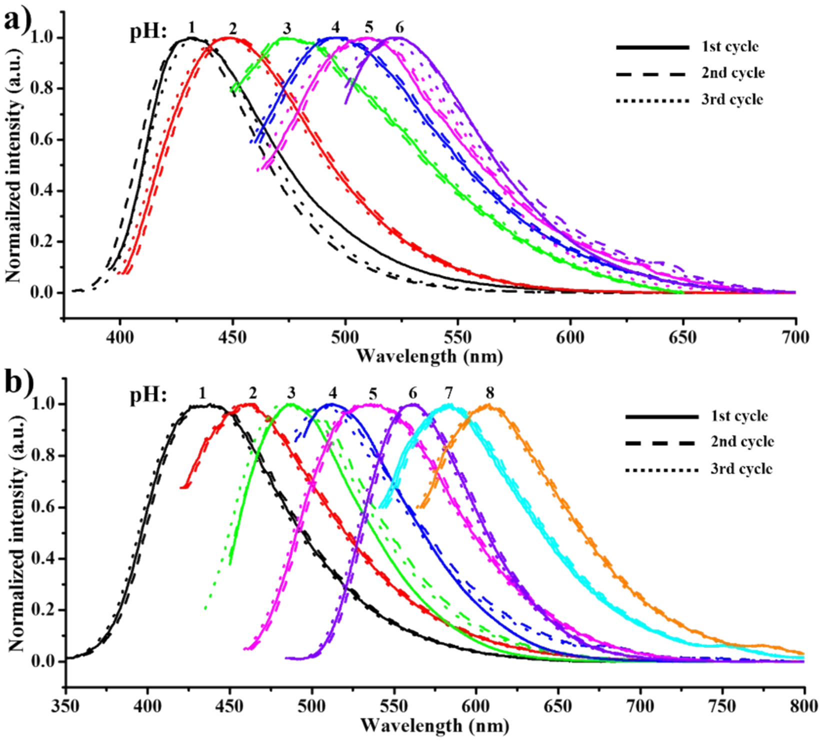

Figure S40. The pH dependent fluorescence spectra of BUT-62 (a) and -63 (b) recorded in repeat tests for 3 cycles.

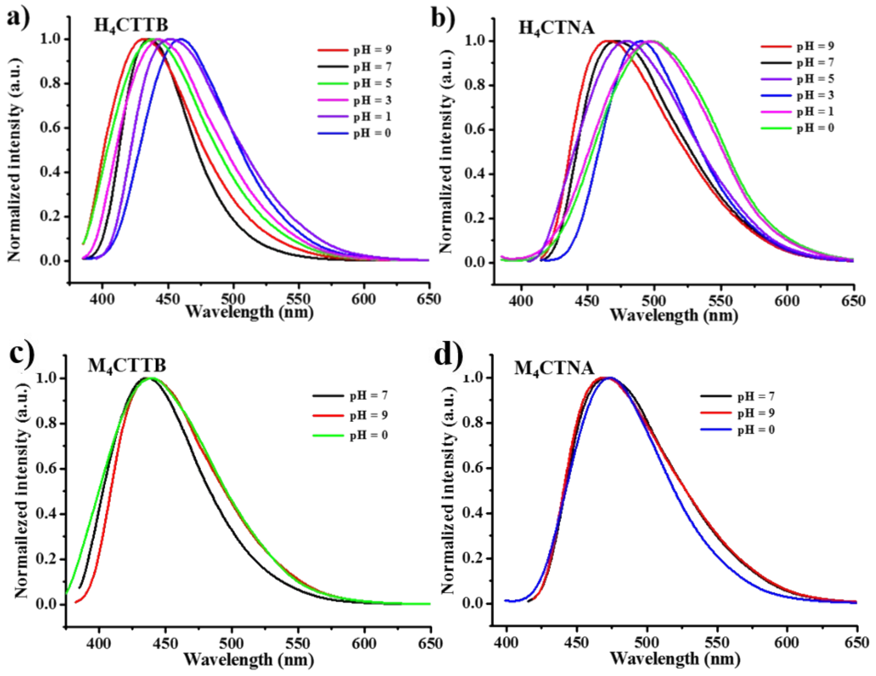

Figure S41. Intensity normalized fluorescence spectra of H$_4$CTTB (a), H$_4$CTNA (b), M$_4$CTTB (c) and M$_4$CTNA (d) ligands dissolved in water with different pH values. respectively.

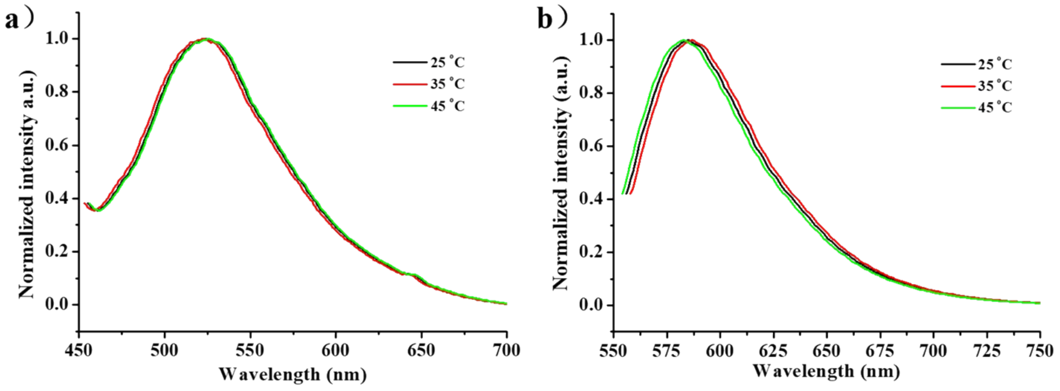

Figure S42. Intensity normalized fluorescence spectra of BUT-62 (a) and BUT-63 (b) at pH = 7 and different temperatures.

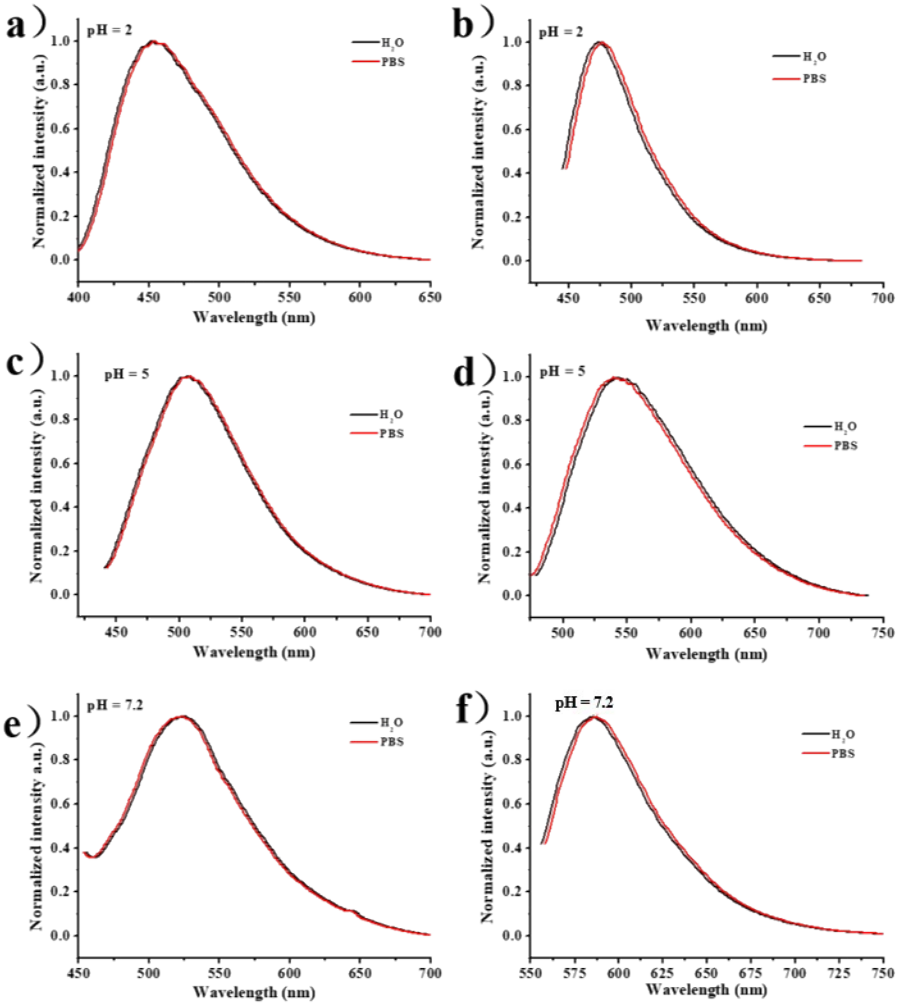

Figure S43. Intensity normalized fluorescence spectra of BUT-62 (a, c, and e) and BUT-63 (b, d, f) at pH = 2, 5, and 7.2 with different ionic strength.

Supplementary Tables

Table S1. Crystal data and structural refinement of BUT-62W, for atomic coordinates, equivalent isotropic displacement parameters, bond lengths, angles, and anisotropic displacement parameters pleasesee the CIF.

Compound name	BUT-62W
Empirical formula	$Zr_6O_{38.5}H_{99.0}C_{97.0}N_{7.5}$
Formula weight	2533.20
Temperature (K)	100(10)
Crystal system	Orthorhombic
Space group	*Immm*
a (Å)	21.5952(9)
b (Å)	31.5124(8)
c (Å)	33.4712(1)
α (°)	90
β (°)	90
γ (°)	90
V(Å^3)	22777.7(1)
Z	8
Calculated density (mg/m^3)	0.610
F(000)	4128
Index ranges	$–26 \le h \le 26$, $–28 \le k \le 38$, $–34 \le l \le 41$
θ range for data collection	3.624 –65.080
Reflections collected	58361
Independent reflections	10339 [R(int) = 0.1209]
Data/restraints/parameters	10339/0/286
Goodness-of-fit on F^2	1.075
Final R indices [$I > 2\sigma(I)$]	$R_1^a = 0.0505$, $wR_2^b = 0.1267$
R indices (all data)	$R_1^a = 0.0870$, $wR_2^b = 0.1399$
Largest diff. peak and hole (e/Å^3)	0.948/-1.122

^{a} $R_1 = \Sigma(||F_0|-|F_C||)/\Sigma|F_0|$.

^{b} $wR_2 = [\Sigma w(|F_0|^2-|F_C|^2)^2/\Sigma w(F_0{}^2)]^{1/2}$

Table S2. Crystal data and structural refinement of BUT-62Y, for atomic coordinates, equivalent isotropic displacement parameters, bond lengths, angles, and anisotropic displacement parameters please see the CIF.

Compound name	BUT-62Y
Empirical formula	$Zr_6O_{52}H_{97}C_{80}N_2$
Formula weight	2465.95
Temperature (K)	100(10)
Crystal system	Orthorhombic
Space group	*Immm*
a (Å)	17.723(5)
b (Å)	32.705(3)
c (Å)	34.670(4)
α (°)	90
β (°)	90
γ (°)	90
V(Å^3)	20096(6)
Z	8
Calculated density (mg/m^3)	0.691
F(000)	4128
Index ranges	$-20 \leq h \leq 19, -38 \leq k \leq 32, -40 \leq l \leq 39$
θ range for data collection	3.716 –65.073
Reflections collected	39298
Independent reflections	9189 [R(int) = 0.3270]
Data/restraints/parameters	9189/271/286
Goodness-of-fit on F^2	1.052
Final R indices [$I > 2\sigma(I)$]	$R_1{}^a = 0.1153$, $wR_2{}^b = 0.2145$
R indices (all data)	$R_1{}^a = 0.2695$, $wR_2{}^b = 0.2653$
Largest diff. peak and hole (e/Å^3)	1.428/-1.1598

$^a R_1 = \Sigma(||F_0|-|F_C||)/\Sigma|F_0|$.

$^b wR_2 = [\Sigma w(|F_0|^2-|F_C|^2)^2/\Sigma w(F_0{}^2)]^{1/2}$

Table S3. Crystal data and structural refinement of BUT-62Y-H_2O (BUT-62Y with water molecules strongly interacted with the framework), for atomic coordinates, equivalent isotropic displacement parameters, bond lengths, angles, and anisotropic displacement parameters please see the CIF.

Compound name	BUT-62Y-H_2O (BUT-62Y with water molecules strongly interacted with the framework)
Empirical formula	$Zr_6O_{52}H_{97}C_{80}N_2$
Formula weight	2465.95
Temperature (K)	100(2)
Crystal system	Orthorhombic
Space group	*Immm*
a (Å)	17.723(5)
b (Å)	32.705(3)
c (Å)	34.670(4)
α (°)	90
β (°)	90
γ (°)	90
V(Å^3)	20096(6)
Z	8
Calculated density (mg/m^3)	0.781
F(000)	4672
Index ranges	$-20 \leq h \leq 19$, $-38 \leq k \leq 32$, $-40 \leq l \leq 39$
θ range for data collection	3.716–65.073
Reflections collected	41465
Independent reflections	9189 [R(int) = 0.3270]
Data/restraints/parameters	9189/310/320
Goodness-of-fit on F^2	1.019
Final R indices [$I > 2\sigma(I)$]	$R_1^a = 0.1339$, $wR_2^b = 0.2853$
R indices (all data)	$R_1^a = 0.2921$, $wR_2^b = 0.3539$
Largest diff. peak and hole (e/Å^3)	1.274/-1.767

[a] $R_1 = \Sigma(||F_0|-|F_C||)/\Sigma|F_0|$.

[b] $wR_2 = [\Sigma w(|F_0|^2-|F_C|^2)^2/\Sigma w(F_0^2)]^{1/2}$

Table S4. Crystal data and structural refinement of Toulene@BUT-62, for atomic coordinates, equivalent isotropic displacement parameters, bond lengths, angles, and anisotropic displacement parameters pleasesee the CIF.

Compound name	Toluene@BUT-62
Empirical formula	$Zr_6C_{122}H_{106}N_2O_{32}$
Formula weight	2659.49
Temperature (K)	100(10)
Crystal system	Orthorhombic
Space group	*Immm*
a (Å)	22.2490(6)
b (Å)	31.0425(8)
c (Å)	33.0217(7)
α (°)	90
β (°)	90
γ (°)	90
V(Å^3)	22806.9(1)
Z	8
Calculated density (mg/m^3)	0.609
F(000)	4128
Index ranges	$-26 \leq h \leq 23$, $-37 \leq k \leq 36$,$-39 \leq l \leq 21$
θ range for data collection	3.625–67.072
Reflections collected	34915
Independent reflections	10851[R(int) = 0.0846]
Data/restraints/parameters	10851/6/286
Goodness-of-fit on F^2	1.002
Final R indices [$I > 2\sigma(I)$]	$R_1{}^a = 0.0780$, $wR_2{}^b = 0.2297$
R indices (all data)	$R_1{}^a = 0.1044$, $wR_2{}^b = 0.2549$

$^a R_1 = \Sigma(||F_0|-|F_C||)/\Sigma|F_0|$.

$^b wR_2 = [\Sigma w(|F_0|^2-|F_C|^2)^2/\Sigma w(F_0{}^2)]^{1/2}$

Table S5. Crystal data and structural refinement of BUT-62W-CH_3, for atomic coordinates, equivalent isotropic displacement parameters, bond lengths, angles, and anisotropic displacement parameters please see the CIF.

Compound name	BUT-62W-CH_3
Empirical formula	$Zr_6O_{37}H_{94.5}C_{95.5}N_{6.5}$
Formula weight	2472.64
Temperature (K)	100(10)
Crystal system	Orthorhombic
Space group	*Immm*
a (Å)	21.5420(7)
b (Å)	32.0006(9)
c (Å)	33.1723(6)
α (°)	90
β (°)	90
γ (°)	90
V(Å^3)	22867.6(11)
Z	8
Calculated density (mg/m^3)	0.615
F(000)	4192
Index ranges	$-13 \leq h \leq 25$, $-38 \leq k \leq 36$,$-39 \leq l \leq 39$
θ range for data collection	3.636–66.591
Reflections collected	34252
Independent reflections	10756[R(int) = 0.0698]
Data/restraints/parameters	10756/288/292
Goodness-of-fit on F^2	0.948
Final R indices [$I > 2\sigma(I)$]	$R_1{}^a = 0.0517$, $wR_2 = 0.1393$
R indices (all data)	$R_1{}^a = 0.0737$, $wR_2 = 0.1515$
Largest diff. peak and hole (e/Å^3)	1.98/-1.19

^{a} $R_1 = \Sigma(||F_0|-|F_C||)/\Sigma|F_0|$.

^{b} $wR_2 = [\Sigma w(|F_0|^2-|F_C|^2)^2/\Sigma w(F_0{}^2)]^{1/2}$

Table S6. Crystal data and structural refinement of BUT-63W, for atomic coordinates, equivalent isotropic displacement parameters, bond lengths, angles, and anisotropic displacement parameters please see the CIF.

Compound name	BUT-63W
Empirical formula	$Zr_6O_{41}H_{123.5}C_{101.0}N_{8.5}$
Formula weight	2659.94
Temperature (K)	100(10)
Crystal system	Orthorhombic
Space group	*Immm*
a (Å)	24.6270(8)
b (Å)	36.7534(10)
c (Å)	39.9531(7)
α (°)	90
β (°)	90
γ (°)	90
V(Å^3)	36162.6(17)
Z	8
Calculated density (mg/m^3)	0.457
Absorption coefficient (mm^{-1})	1.570
F(000)	4944
Index ranges	$-29 \leq h \leq 28, -43 \leq k \leq 40, -47 \leq l \leq 46$
θ range for data collection	3.53–66.593
Reflections collected	54415
Independent reflections	16870[R(int) = 0.1030]
Data/restraints/parameters	16870/169/358
Goodness-of-fit on F^2	1.041
Final R indices [$I > 2\sigma(I)$]	$R_1{}^a = 0.0698$, $wR_2 = 0.1656$
R indices (all data)	$R_1{}^a = 0.1402$, $wR_2 = 0.1929$
Largest diff. peak and hole (e/Å^3)	0.86/-0.76

[a] $R_1 = \Sigma(||F_0|-|F_C||)/\Sigma|F_0|$.

[b] $wR_2 = [\Sigma w(|F_0|^2-|F_C|^2)^2/\Sigma w(F_0{}^2)]^{1/2}$

Table S7. Summary ofreported Zr-MOFs constructed with tetratopic ligands.

Zr-MOF	Ligand	Zr cluster/core	Topology
NU-1100[5]	$PTBA^{4-}$	$Zr_6(\mu_3\text{-O})_4(\mu_3\text{-OH})_4$	**ftw**, (4,12)-connected
NU-1101[6]	$Py\text{-}XP^{4-}$	$Zr_6(\mu_3\text{-O})_4(\mu_3\text{-OH})_4$	**ftw**, (4,12)-connected
NU-1102[7]	$Por\text{-}PP^{4-}$	$Zr_6(\mu_3\text{-O})_4(\mu_3\text{-OH})_4$	**ftw**, (4,12)-connected
NU-1103[6]	$Py\text{-}PTP^{4-}$	$Zr_6(\mu_3\text{-O})_4(\mu_3\text{-OH})_4$	**ftw**, (4,12)-connected
NU-1104[6]	$Por\text{-}PTP^{4-}$	$Zr_6(\mu_3\text{-O})_4(\mu_3\text{-OH})_4$	**ftw**, (4,12)-connected
MOF-525[7]	$TCPP^{4-}$	$Zr_6(\mu_3\text{-O})_4(\mu_3\text{-OH})_4$	**ftw**, (4,12)-connected
MOF-535[7]	XF^{4-}	$Zr_6(\mu_3\text{-O})_4(\mu_3\text{-OH})_4$	**ftw**, (4,12)-connected
PCN-94[8]	$ETTC^{4-}$	$Zr_6(\mu_3\text{-O})_4(\mu_3\text{-OH})_4$	**ftw**, (4,12)-connected
PCN-221[9]	$TCPP^{4-}$	$Zr_8(\mu_4\text{-O})_6$	**ftw**, (4,12)-connected
PCN-228[10]	$TCP\text{-}1^{4-}$	$Zr_6(\mu_3\text{-O})_4(\mu_3\text{-OH})_4$	**ftw**, (4,12)-connected
PCN-229[10]	$TCP\text{-}2^{4-}$	$Zr_6(\mu_3\text{-O})_4(\mu_3\text{-OH})_4$	**ftw**, (4,12)-connected
PCN-230[10]	$TCP\text{-}3^{4-}$	$Zr_6(\mu_3\text{-O})_4(\mu_3\text{-OH})_4$	**ftw**, (4,12)-connected
CPM-99[11]	$TCBPP^{4-}$	$Zr_6(\mu_3\text{-O})_4(\mu_3\text{-OH})_4$	**ftw**, (4,12)-connected
Zr-BTBA[12]	$BTBA^{4-}$	$Zr_6(\mu_3\text{-O})_4(\mu_3\text{-OH})_4$	**ftw**, (4,12)-connected
Zr-PTBA[12]	$PTBA^{4-}$	$Zr_6(\mu_3\text{-O})_4(\mu_3\text{-OH})_4$	**ftw**, (4,12)-connected
NU-1105[13]	$Py\text{-}FP^{4-}$	$Zr_6(\mu_3\text{-O})_4(\mu_3\text{-OH})_4$	**ftw**,(4,12)-connected
PCN-223[14]	$TCPP^{4-}$	$Zr_6(\mu_3\text{-O})_4(\mu_3\text{-OH})_4$	**shp**, (4,12)-connected
NU-902[15]	$TCPP^{4-}$	$Zr_6(\mu_3\text{-O})_4(\mu_3\text{-OH})_4$	**scu**,(4,8)-connected
NUPF-1[16]	$L1^{4-}$	$Zr_6(\mu_3\text{-O})_4(\mu_3\text{-OH})_4$	**scu**,(4,8)-connected
PCN-128[17]	$ETTC^{4-}$	$Zr_6(\mu_3\text{-OH})_8$	**csq**,(4,8)-connected
MMPF-6[18]	$TCPP^{4-}$	$Zr_6(\mu_3\text{-O})_8$	**csq**, (4,8)-connected
PCN-222[19]	$TCPP^{4-}$	$Zr_6(\mu_3\text{-OH})_8$	**csq**, (4,8)-connected
MOF-545[7]	$TCPP^{4-}$	$Zr_6(\mu_3\text{-O})_8$	**csq**, (4,8)-connected
NU-1000[20]	$TBAPy^{4-}$	$Zr_6(\mu_3\text{-OH})_8$	**csq**, (4,8)-connected
PCN-224[21]	$TCPP^{4-}$	$Zr_6(\mu_3\text{-O})_4(\mu_3\text{-OH})_4$	**she**, (4,6)-connected
PCN-225[22]	$TCPP^{4-}$	$Zr_6(\mu_3\text{-O})_4(\mu_3\text{-OH})_4$	**sqc**, (4,8)-connected

Table S8. Distances between H-bonding donor-acceptor atoms in BUT-62W and BUT-62Y.

	H-bonding Donor-acceptor	Distances in BUT-62W	Distances in BUT-62Y
1	N^{I}-O^{I}	3.00 Å	2.75 Å
2	O^{II}-O^{III}	3.18 Å	2.42 Å
3	O^{II}-O^{IV}	3.07 Å	2.27 Å

Table S9. Calculated HOMO and LUMO energy levels for the H_4CTTB ligand in different states.

	HOMO(ev)	LUMO(ev)	Band Gap(ev)
H_4CTTB(configuration as in BUT-62W)	-4.837	-2.180	2.657
H_4CTTB(configuration as in BUT-62Y)	-4.532	-2.465	2.067
H_4CTTB(free acid)	-4.508	-2.156	2.352
H_4CTTB(configuration as in Toluene@BUT-62)	-4.925	-2.209	2.716

References

(1) H. Huang, Q. Fu, B. Pan, S. Zhuang, L. Wang, J. Chen, D. Ma, C. Yang, *Org. Lett.,* 2012, **14**, 4786-4789.

(2) CrysAlis RED, version 1.171.32.38, SCALE3 ABSPACK scaling algorithm; Oxford Diffraction Ltd.: Blacksburg, Virginia (2013).

(3) Sheldrick GM (1997) SHELXTL NT Version 5.1, Program for Solution and Refinement of Crystal Structures, University of Göttingen: Germany.

(4) Spek AL (2003) Single-crystal structure validation with the program PLATON. *J. Appl. Crystallogr.,* **36***,* 7-13.

(5) O. V. Gutov, W. Bury, D. A. Gómez-Gualdrón, V. Krungleviciute, D. Fairen-Jimenez, J. E. Mondloch, A. A. Sarjeant, S. S. Al-Juaid, R. Q. Snurr, J. T. Hupp, T. Yildirim, O. K. Farha, *Chem.-Eur. J.,* 2014, **20**, 12389-12393.

(6) T. C. Wang, W. Bury, D. A. Gómez-Gualdrón, N. A. Vermeulen, J. E. Mondloch, P. Deria, K. Zhang, P. Z. Moghadam, A. A. Sarjeant, R. Q. Snurr, J. F. Stoddart, J. T. Hupp, O. K. Farha, *J. Am. Chem. Soc.*, 2015, **137**, 3585-3591.

(7) W. Morris, B. Volosskiy, S. Demir, F. Gándara, P. L. McGrier, H. Furukawa, D. Cascio, J. F. Stoddart, O. M. Yaghi, *Inorg. Chem.,* 2012, **51**, 6443-6445.

(8) Z. Wei, Z.-Y. Gu, R. K. Arvapally, Y.-P. Chen, R. N. McDougald, J. F. Ivy, A. A. Yakovenko, D. Feng, M. A. Omary, H.-C. Zhou, *J. Am. Chem. Soc.,* 2014, **136**, 8269-8276.

(9) D. Feng, H.-L. Jiang, Y.-P. Chen, Z.-Y. Gu, Z. Wei, H.-C. Zhou, *Inorg. Chem.,* 2013, **52**, 12661-12667.

(10) T.-F. Liu, D. Feng, Y.-P. Chen, L. Zou, M. Bosch, S. Yuan, Z. Wei, S. Fordham, K. Wang, H.-C. Zhou, *J. Am. Chem. Soc.,* 2015, **137**, 413-419.

(11) Q. Lin, X. Bu, A. Kong, C. Mao, X. Zhao, F. Bu, P. Feng, *J. Am. Chem. Soc.*, 2015, **137**, 2235-2238.

(12) S. B. Kalidindi, S. Nayak, M. E. Briggs, S. Jansat, A. P. Katsoulidis, G. J. Miller, J. E. Warren, D. Antypov, F. Cora, B. Slater, M. R. Prestly, C. Marti-Gastaldo, M. J. Rosseinsky, *Angew. Chem. Int. Ed.*, 2015, **54**, 221-228.

(13) P. Deria, D. A. Gómez-Gualdrón, W. Bury, H. T. Schaef, T. C. Wang, P. K. Thallapally, A. A. Sarjeant, R. Q. Snurr, J. T. Hupp, Farha, O. K. *J. Am. Chem. Soc.,*2015, **137**, 13183-13190.

(14) D. Feng, Z.-Y. Gu, Y.-P. Chen, J. Park, Z. Wei, Y. Sun, M. Bosch, S. Yuan, H.-C. Zhou, *J. Am. Chem. Soc.*, 2014, **136**, 17714-17717.

(15) P. Deria, D. A. Gomez-Gualdron, I. Hod, R. Q. Snurr, J. T. Hupp, O. K. Farha, *J. Am. Chem. Soc.*, 2016, **138**, 14449-14457.

(16) L. Xu, Y.-P. Luo, L. Sun, Y. Xu, Z.-S. Cai, M. Fang, R.-X. Yuan, H.-B. Du, *Chem.-Eur. J.*, 2016, **22**, 6268-6276.

(17) Q. Zhang, J. Su, D. Feng, Z. Wei, X. Zou, H. -C. Zhou, *J. Am. Chem. Soc.*, 2015, **137**, 10064-10067.

(18) Y. Chen, T. Hoang, S. Ma, *Inorg. Chem.*, 2012, **51**, 12600-12602.

(19) D. Feng, Z.-Y. Gu, J.-R. Li, H.-L. Jiang, Z. Wei, H.-C. Zhou, *Angew. Chem. Int. Ed.*, 2012, **124**, 10307-10310.

(20) J. E. Mondloch, W. Bury, D. Fairen-Jimenez, S. Kwon, E. J. DeMarco, M. H. Weston, A. A. Sarjeant, S. T. Nguyen, P. C. Stair, R. Q. Snurr, O. K. Farha, J. T. Hupp, *J. Am. Chem. Soc.,*2013, **135**, 10294-10297.

(21) D. Feng, W.-C. Chung, Z. Wei, Z.-Y. Gu, H.-L. Jiang, Y.-P. Chen, D. J. Darensbourg, H.-C. Zhou, *J. Am. Chem. Soc.*, 2013, **135**, 17105-17110.

(22) H.-L. Jiang, D. Feng, K. Wang Z.-Y., Gu, Z. Wei, Y.-P. Chen, H.-C. Zhou, *J. Am. Chem. Soc.*, 2013, **135**, 13934-13938.